

OUTPUT 2	Design of new drug-drug compound combinations
Project specific objective	1) Innovative pharmaceutical formulations and technologies
Output description	Design of new drug – drug compound combinations (TRL5). The approach should include molecular modelling of novel compounds to identify novel cocrystal pairs and synthesized using a range of processing technologies.
Project Output Target	Targeted : 2 ; Achieved : 4 Overachievement: Four cocrystalline products (Product #1: Perampanel – Saccharin; Product #2: Apixaban – Oxalic Acid, Product #3: Rivaroxaban – Hesperitin and Product #4: Carbamazepine – Naproxen) have been designed instead of two products as initially planned.
Expected project specific result (s)	The manufacturing of two products made of multicomponent drug – drug. Active ingredients with optimized solubility (expected gain 60%) and stability (expected gain 90%) properties. The delivered products will be patented and ready to use in pharmaceutical applications. They will increase the competitiveness of SMEs.
Partner responsible	PP7 (University of Greenwich) & PP10 (Cubic Pharmaceuticals)
Other Partners involved	LP12 (University of Lille), PP5 (University of East Anglia)
Summary of the objectives, activities and achievements obtained during the project	
<p>There are 6 Deliverables which compose the Output 2 as follow. These reflect the key objectives of Output 2.</p> <ul style="list-style-type: none"> A) D 1.2.1. Physical characterization and manipulation of single compounds and multicomponent drug (report submitted) B) D 1.2.2. 3D printing process for manufacturing of solid pharmaceutical products (report submitted) C) D 1.2.3. Formulation design and manufacturing of developed products (report submitted) D) D 1.2.4. Method transfer, validation, and manufacturing (delayed – see major modification request) E) D 1.2.5. Filed patent application F) D 1.2.6. Granted Patent <p>Activities:</p> <p>Research: Research work has been conducted in collaboration between PP5, PP7, PP10 and LP12. Two full time and one part – time PDRAs, throughout the duration of the project, have been appointed to work under the guidance of Prof Douroumis (PP7) and Mr Bhatt (PP10). One PhD has been recruited to work under the supervision of Prof. Affouard and Dr. Correia (LP12). Both PP7 and PP10 have focused their research in 3d printing processes (D1.2.2) and design/manufacturing of novel pharmaceutical cocrystals (D 1.2.3, D 1.2.4., D1.2.5). Physical characterizations of materials and design of cocrystals by milling and liquid assisted solvents have been performed by LP12 (D 1.2.1 and D 1.2.5). Physical characterization by NMR have been performed by PP5 (D 1.2.1). All deliverables have been completed awaiting now for the patents to be granted.</p> <p>Industrial and stakeholder engagement: the IMODE team has been actively reach out to the industrial users of the technologies developed in O2 through conferences, exhibitions, company face-to-face visits. As a result of such interaction and outreach effort, PP7 has established a two – year collaboration with a world leading pharmaceutical company on the development of oral pharmaceutical dosage forms. In addition, the collaborative work of PP7 and PP10 resulted in additional funding from the Knowledge Partner Partnerships (INNOVATE UK) for a two-year project in the scale – up of pharmaceutical products using Hot Melt Extrusion.</p>	

Training: PP5, PP7, PP10, and LP12 have visited a wide range of companies and universities to communicate our technologies and provide training to their staff/students. The two PDRAs employed on this output by PP7 and PP10 have already been appointed by Cubic Pharmaceuticals (PP10) while the third has been appointed by HMRA in UK. The PhD student recruited by LP12 has defended her PhD in Dec 2020.

The achievements can be categorised into:

Knowledge: Created/Increased skill and capacities

A) Development of 2 new novel processes for the synthesis of pharmaceutical cocrystals with improved stability and physicochemical characteristics:

Process #1: Supercritical Fluid Processing (SF) to develop Pharmaceutical Salts

Process #2: High Pressure Homogenization (HPH) to develop Nano – Cocrystals

B) Design of 4 novel pharmaceutical products with improved stability and dissolution rates :

Product #1: Perampanel – Saccharin cocrystal (using Hot Melt Extrusion processing, Ball Milling and High-Pressure Homogenization)

Product #2: Apixaban – Oxalic Acid cocrystal (using Hot Melt Extrusion processing, Ball Milling and High-Pressure Homogenization)

Product #3: Rivaroxaban – Hesperitin cocrystal(using Hot Melt Extrusion processing, Ball Milling and High-Pressure Homogenization)

Product #4: Carbamazepine – Naproxen cocrystal (using Ball Milling)

Socio-Economic: Increased business activities/capacities (new products, processes, services, techniques)

The developed technology will be adopted and included in Cubic's portfolio so they can be used in future drug product development and hence increase the company's competitiveness. In addition, three newly synthesized cocrystals will be potentially marketed by Cubic or licenced to other pharmaceutical companies and hence enhance the company's annual turnover.

Socio-Economic: Patent application

2 Patents have been filled on the 2 novel technological processes (see above):

- Preparation of pharmaceutical salt by super critical fluid processing PATENT REF: TXR/BOB/90825GB1) (see Process #1 above)
- Particle size engineering of pharmaceutical salts by high-pressure homogenisation. (PATENT REF: TXR/BOB/90824GB1 [VS.FID2391009]) (see Process #2 above)

1 patent will be filed as soon the agreement between PP7 UoG & PP10 Cubic Pharm is signed:

- Perampanel based Cocrystals (see product#1 above)
- Apixaban based Cocrystals (see product#2 above)

1 Invention disclosure has been submitted to the Tech Transfert Accelerator Network SATT-NORD (French side) on the Carbamazepine – Naproxen cocrystalline system (see product#4 above)

Overachievement in terms of Outputs delivered: Four cocrystalline products (Product #1: Perampanel – Saccharin; Product #2: Apixaban – Oxalic Acid, Product #3: Rivaroxaban – Hesperitin and Product #4: Carbamazepine – Naproxen) have been designed instead of two products as initially planned.

The report is organized as follows:

I) Description of the scientific and technological achievements

A) Development of 2 new novel processes for the synthesis of pharmaceutical cocrystals with improved stability and physicochemical characteristics:

- Process#1 : Supercritical Fluid Processing (SF)
- Process#2 : High Pressure Homogenization (HPH)

B) Design of 4 novel pharmaceutical cocrystal compounds with improved stability and dissolution rates various processing techniques :

- 1) Product#1 : Perampanel – Saccharin cocrystal
- 2) Product#2 : Rivaroxaban – Hesperitin cocrystal
- 3) Product#3 : Apixaban – Oxalic Acid cocrystal
- 4) Product#4 : Carbamazepine – Naproxen cocrystal

C) Design of others cocrystalline compounds using liquid assisted grinding and solution evaporation (Carbamazepine– DL-tartaric acid, Carbamazepine – L-tartaric acid)

D) Development of new computational approaches for the screening of cofomers for cocrystals screening

II) Description of the results obtained for the output in term of specific results category and specific result type

I) Description of the scientific and technological achievements

A) Development of 2 new novel processes for the synthesis of pharmaceutical cocrystals with improved stability and physicochemical characteristics (Supercritical Fluid Processing (SF) and High Pressure Homogenization (HPH))

Introduction

Solubility is a long standing hurdle in drug development with a reported 60% of the newly discovered drugs in recent years are suffering from aqueous solubility issues^{1,2,4}. because of this a great deal of effort is being made by researchers from academic and industry to modify APIs to enhance their solubility without affecting their pharmacological properties. Methods of achieving this include; multicomponent product formation, particle size reduction, solid dispersion, nanosuspension, inclusion complex formation based technique, micellar solubilisation, crystal engineering and many more^{1,3,5}. One of the more popular routs is combining the API with another product to form a multicomponent product, and of this rout salt formation) is one of the simplest and effective processes to address the solubility problem of the API, especially for the ionisable compounds⁶. Salt formation is achieved through selecting an appropriate counter ion for the ionisable drugs through computational and experimental screening and processing the API and counter ion via salt processing methods which can include; solvent evaporation, slurry crystallization, mechanochemical processing, antisolvent preparation, extrusion and super critical fluid processing⁷. Super critical fluids (SCFs) processing is an emerging technique for salification, which is gaining more industrial attention due to it being an organic chemical free process of salt production, thus reducing its environmental impact⁸. Super critical fluids refer to a substance at a temperature and pressure above their critical point, where phase boundaries vanish and liquid and vapour phases coexist. Although there are a variety of SCFs which have been investigated, CO₂ is the most commonly used and offers a number of distinct advantages, such as being non-toxic, non-corrosive, readily available, inexpensive and environment friendly⁹. SCF processing has been used for the multicomponent product formation of pharmaceutical cocrystals¹⁰ in the past.

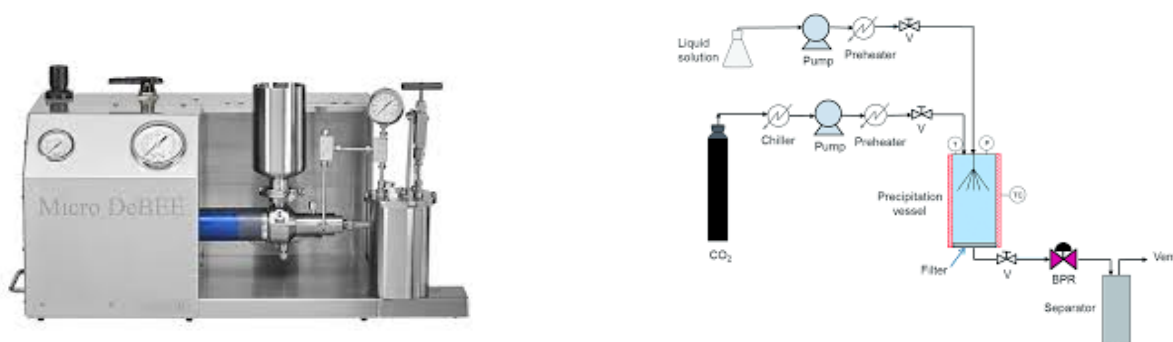


Fig. 1: a) a high pressure homogenizer used for the synthesis of nano-cocrystals and b) schematic diagram of a supercritical device showing the synthesis of pharmaceutical salts

High pressure homogenization (HPH) is a purely mechanical process where solvated raw materials are introduced into a sample holder and then forced through the narrow gap of a homogenising nozzle at high pressures (using a high-pressure pump) of either 150-200 MPa or 350-400 MPa (ultra-high-pressure homogenization). A high-pressure homogenizer consists of a pump which is responsible for compressing the crude fluid to the required pressure and a nozzle for the efficiency of disruption for emulsions prepared with the high-pressure homogenization^{11,12}. Air-driven piston pumps cycle the solution around the homogeniser and back into feeding vessel of the machine to be recycled. The fluidic product is subject to very high shear stress which causes the formation of very fine droplets. This shear is originated from the sudden restriction of the flow under high pressure through a restrictive valve. The high shear stress of the process due to the attainment of turbulent flow conditions and

cavitation phenomena¹³ induces the formation of supramolecular synthons and the nucleation of co-crystals. Extreme high pressure is needed to form the nanoparticles as higher shear is needed for the deformation and breakdown of the particles. For nanoparticles or nanoemulsions, high amounts of surfactants are required for their stabilization due to their high surface to volume ratio. Droplet size decreases mean surface to volume ratio increases. The high pressures, alongside shear effects of mechanical energy conversion into heat, increase the temperature of solutions in the homogenizer. As such, thermostats are used which regulate the temperature of the solution in the machine. HPH typically produces micro-scale crystals but can produce nano-scale crystals through increases in shear pressure and energy input. Shear pressure is controlled by the homogenising nozzle, which produces different levels of shear depending on their type. Multiple other operating conditions, such temperature, processing time, stirring rate of the solution and flow rate are also modifiable, leading to the ability to change and tune product particle size as desired¹³.

The report presents two sections that have been delivered. In Section I we will present the developed supercritical technology for the formation of pharmaceutical salts (**Deliverable 1.2.3**) and in Section II the second processing method for the synthesis of pharmaceutical cocrystals in nanoscale (**Deliverable 1.2.3**)

Experimental Section

Materials

Ketoconazole (KTZ), carbamazepine (CBZ), oxalic acid and saccharin were purchased from Sigma-Aldrich (Gillingham, UK). The purity of these chemicals was more than 99%. Solvents (reagent grade methanol, acetone and HPLC grade methanol) were purchased from Fisher Chemicals (Loughborough, UK). Liquid carbon di oxide was supplied by BOC Ltd. All the solid materials and solvents were used as received.

High pressure homogenization

Crystallization of ketoconazole - oxalic acid was formed by high-pressure homogenisation (Fig. 1a). Specifically, a mixture of ketoconazole and oxalic acid (molar stoichiometric ratio 1:1.1) were dissolved in 50 ml of a solvent mixture of acetone and methanol (1:1). The role of various polymers as stabilisers was investigated. For this purpose, 0.25% to 0.5% (w/v) of polymers were added to the mixture. After the addition of polymer, the resulting clear solution was rapidly transferred and homogenized in a Micro Debee laboratory homogeniser (South Easton, MA, USA) at 15000 psi for a predetermined time at room temperature. Selected formulations were used again in the homogenization process after applying temperature 40°C for the same period. At the end of the homogenization process, the solid was separated by filtration under vacuum. To collect the particles with size even in nanoscale, filters with pore size 100 nm (Millipore, nylon filters) were used. The filtrate was dried overnight at 50°C and stored for further analysis.

Supercritical fluid processing

Both the API (Ketoconazole) and the salt former (oxalic acid) were dissolved in a mixture of solvents and the resulting solution was processed by scCO₂ under a specific temperature (31.3°C) and pressure environment (100bar). Several single crystals were grown when the solution was exposed in a chamber (Fig. 1b) filled with scCO₂ and solid powder was formed when the drug-former solution was sprayed into the chamber.

Results and discussion

Section I Deliverable 1.2.3

Thermal and XRD analysis

Thermal analysis by DSC was performed to investigate the thermal events occurred in the bulk solid and new solid materials prepared by HPH process. From **Fig. 2a**, the thermal events which occurred in the different samples can be seen. It can be seen that KTZ has a sharp melting point at 150 °C while oxalic acid displayed a melting point at 192 °C. The solid resulting from KTZ: oxalic acid (1:1.1) HPH process showed a unique endothermic peak at 197 °C (**Fig. 2a**). There is no other endothermic event noticed in the processed materials, which indicates the formation of new material compared to parent materials. Comparing with the previously reported KTZ oxalate salt data from *Martin et al.* (2013)¹, KTZ oxalic acid (1:1.1) matches with that of the melting point of KTZ oxalate salt formed by

solution crystallisation method, where the endothermic peak was around 198 °C confirming the formation of KTZ oxalate salt.

The new solid materials resulting from the HPH process along with bulk materials were also subject to PXRD analysis (**Fig. 2b**) to identify the diffraction pattern obtained from each solid. This newly obtained data were compared with the previously reported data from the CSD by using TOPAS analysis software. The percentage of the match between newly obtained crystal data with previously reported data is identified by Rietveld refinement of TOPAS V4.2 (Bruker). Though good fitting depends on the visual fitting of the crystalline peak, it is generally agreed that if the weighted profile R factor (Rwp) is within or around 3 times of the expected R factor (Rexp), the match or refinement is satisfactory (2).

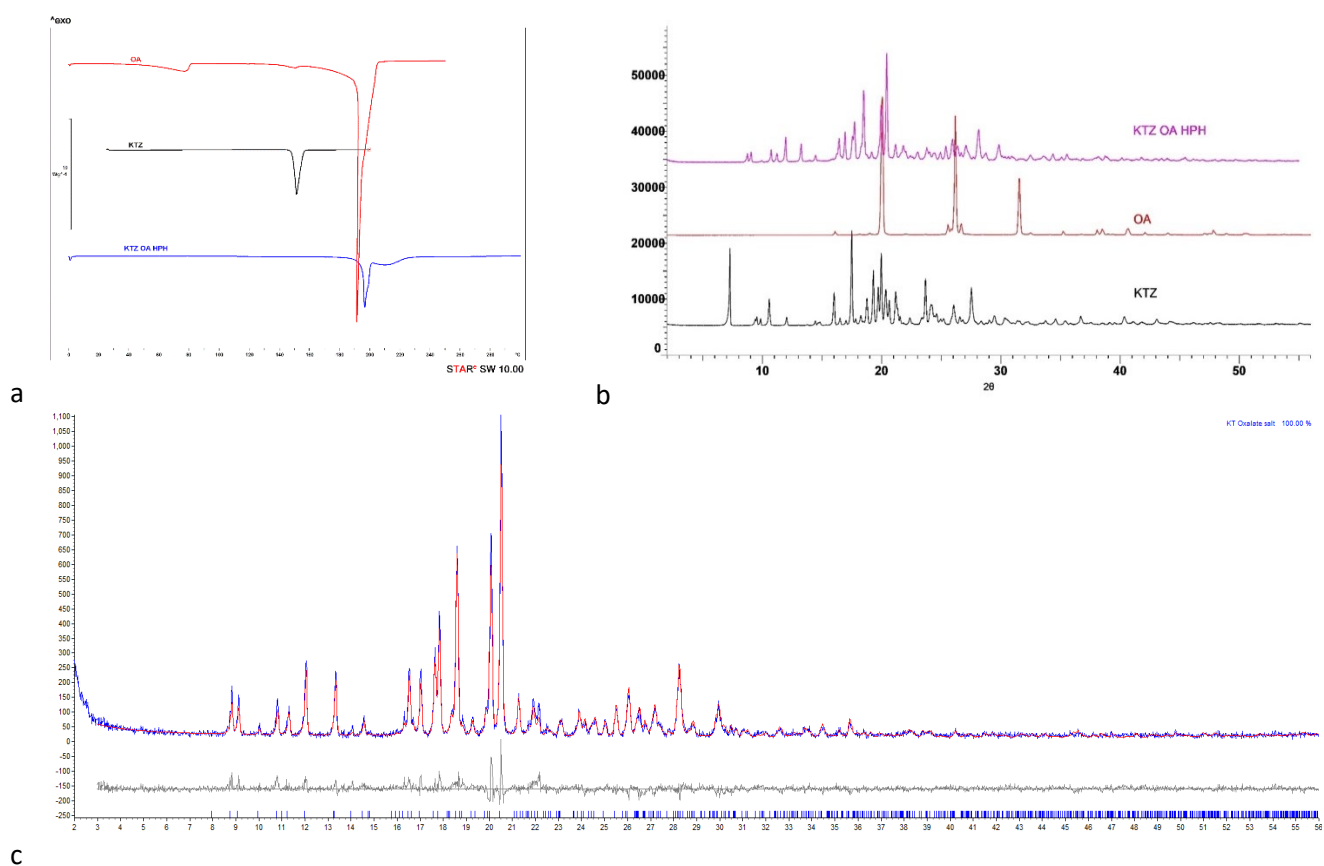


Fig. 2: a) DSC thermograms of bulk KTZ, oxalic acid, and KTZ OA salt prepared by HPH, b) Diffraction pattern of bulk KTZ, bulk OA, and KTZ OA salt prepared by HPH process, c) Rietveld refinement for the homogenized KTZ: OA (1:1.1) presenting the measured pattern (blue line), the simulated pattern (red line) and the difference pattern (grey line).

R-Values: Rexp : 15.02 Rwp : 18.86 Rp : 14.64 GOF : 1.26 // Rexp` : 17.95 Rwp` : 22.53 Rp` : 17.85 DW : 1.35

From **Fig. 2b**, as observed, a distinct crystalline profile was obtained from the KTZ oxalic acid HPH processed solid materials which do not match with the bulk KTZ and oxalic acid crystal data that confirms the formation of a new solid crystal. Furthermore KTZ: oxalic acid crystal diffraction data were compared with the previously reported data by *Martin et al*¹, in the CSD. The similarity between these two data is confirmed by the Rietveld refinement using TOPAS software where Rwp is within two times of Rexp (**Fig. 2c**). The similarity between these newly obtained crystal data and the previously reported data confirms the formation of KTZ oxalic acid salt with a purity close to 100%. After analysing the thermal behaviour and PXRD data of the solids resulting from the HPH process, it can be seen that the KTZ-OA salt formation is possible by HPH process. Furthermore, the same HPH process was performed after adding four different stabilizers (Pharmacoat-606, Ppluronic-F127, Soluplus, and TPGS) in different percentages

(0.25% and 0.50% w/v) in KTZ-OA solution. The new solids obtained after the addition of stabilizers were analysed by DSC. The thermal behaviour of the newly formed solid was similar as before which indicates, that the stabilizer had no impact on the salt formation. PXRD analysis also showed an identical result. Therefore, it has been confirmed that salt formation occurs in each process, regardless of the different types and amount of the stabilizer been used.

Particle sizes were scaled by SEM imaging to find out the differences observed after the addition of different stabilisers in different percentages. After using the PLF127 stabilizer, most changes in crystal size and shape were observed. All the crystals produced here were almost nano range in size and all appeared in the same shape, where minimal deformation was also observed (**Fig. 3**).

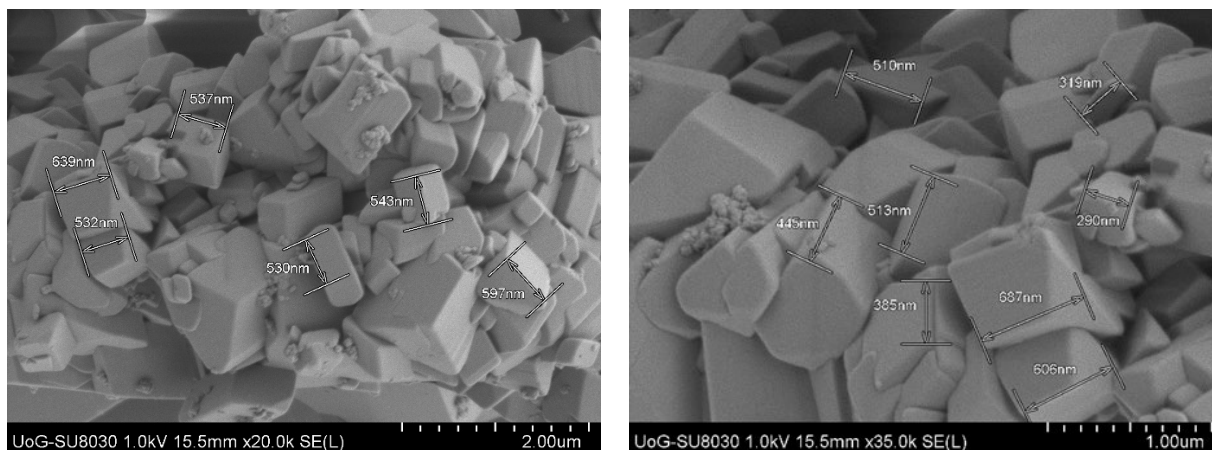


Fig. 3: SEM images of KTZ OA salt produced by HPH process stabilizer, PLF127 at 40 °C.

B. Nano and micro size cocrystal formation

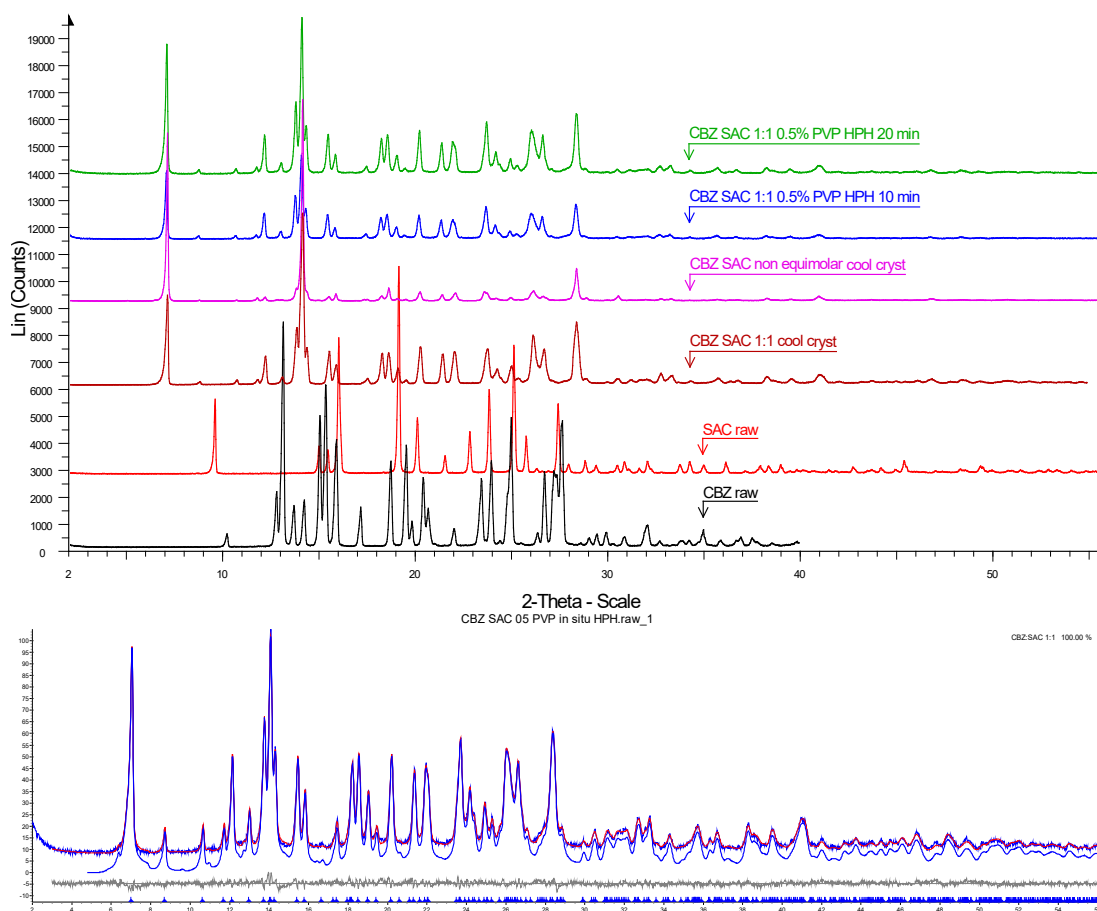
Cocrystals of carbamazepine-saccharin (CBZ-SAC 1:1) and Indomethacin- saccharin (IND-SAC 1:1) were prepared by antisolvent cocrystallisation coupled with high-pressure homogenisation. Specifically, a mixture of CBZ (2 mmol) and SAC (5.28 mmol) was dissolved in 20 mL methanol. Deionised water was used as the antisolvent and was added into the methanol solution (volume ratio of methanol to water was 1:2). After the addition of water, the solution started becoming turbid after approximately 5 minutes. To achieve simultaneous cocrystallisation and particle size reduction, the solution was rapidly transferred and homogenized in a Micro DebEE homogeniser at 15000 psi for 20 minutes at room temperature. The role of various polymers as stabilisers was investigated. For this purpose, 0.5% w/v aqueous solutions of polymers were used as the antisolvent phase. The polymers investigated were the following: PHARMACOAT® 606 (Shin-Etsu, Japan), D-alpha-tocopheryl polyethylene glycol succinate (TPGS, Eastman Chemical Company, USA), Pluronic® F127 and Kollidon® VA 64 (BASF, Germany). At the end of the process, the cocrystals were separated by filtration under vacuum. To collect particles with size even in the nanoscale, filters with a pore size of 0.22 µm were used (MF-Millipore membrane filters). The filtrate was dried overnight at 40 °C and was further characterised by XRPD, DSC, and SEM. A similar procedure was followed for IND-SAC cocrystal formation.

Carbamazepine - saccharin

Bulk materials and all the cocrystals produced using homogenisation with different stabilizers were subjected to PXRD analysis. From **Fig. 4a**, as observed, a distinct crystalline profile was obtained for the HPH processed solid materials which do not match with the bulk CBZ and SAC crystal data that confirms the formation of a new solid crystal. Furthermore, CBZ: SAC crystal diffraction data were compared with the previously reported data in the CSD. The similarity between these two data is confirmed by the Rietveld refinement using TOPAS software where Rwp is within two times of Rexp (**Fig. 4b**). The similarity between these newly obtained crystal data and the previously reported data confirms the formation of CBZ: SAC cocrystal with a purity close to 100%.

Particle sizes were scaled by SEM imaging to find out the differences observed after the addition of different stabilisers in different percentages. When using the PLF127 as stabilizer, several changes in crystal size and shape were observed. Most of the crystals produced at the end of the process were almost nano-range in size and all

appeared in the same shape, where minimal deformation was also observed (Fig. 5).



R-Values

Rexp : 5.00	Rwp : 8.19	Rp : 6.22	GOF : 1.64
Rexp` : 5.87	Rwp` : 9.61	Rp` : 7.49	DW : 0.81

Fig. 4: a) PXRD diffractograms of bulk materials and cocrystal prepared with different stabilisers by high-pressure homogenisation, b) quantitative XRD was conducted using Rietveld refinement and performed with TOPAS version 4.2

Indomethacin – Saccharin cocrystal

The bulk IND displayed a sharp melting peak at 161.0 °C, with SAC showing a step melting point at 229.4 °C, in accordance with the reported thermal behaviour. The thermal profile of the pure IND-SAC cocrystal displays a single endotherm for the melting point of the cocrystal with an absence of any unbound or absorbed solvent or water, eutectic peak and demonstrates the stability of the phase until the melting indicating complete batch cocrystallisation and a high cocrystal purity (Fig 6a).

The synthesis and quality of the IND/SAC cocrystals were further evaluated through XRPD to identify the diffraction patterns of the bulk materials, physical mixture, and unmodified IND/SAC cocrystals. The analysis of bulk IND showed characteristic intensity peaks at 10.25, 11.67, 16.77, 17.02, 19.68, 21.87, 23.99, 26.61° 2θ, while bulk SAC displayed intensity peaks at 9.56, 15.91, 16.02, 17.23, 19.13, 25.14° 2θ (Fig. 6b). The diffractogram for the IND/SAC cocrystals was compared to previously reported structural data published in the CSD (REFCODE: UFERED) (Fig. 6a,b). The newly produced cocrystals were found to be identical to the CSD standard displaying characteristic intensity peaks at 5.43, 10.89, 14.42, 21.22, 25.45, and 27.07° 2θ, with the absence of any peaks for the unreacted bulk components, indicating a high-quality cocrystal.

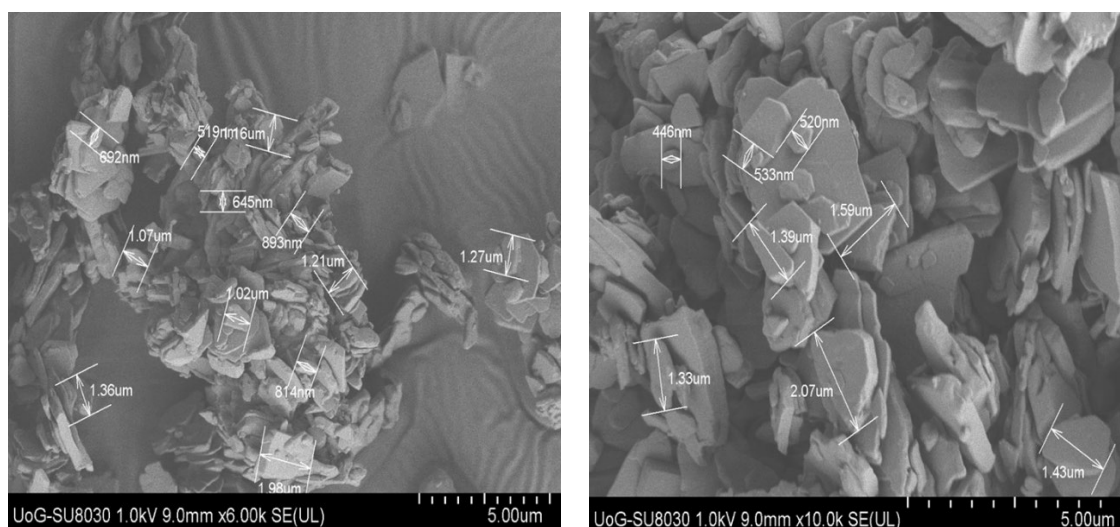


Fig. 5: SEM images of CBZ: SAC (1:1) cocrystals stabilised with 0.5% w/v prepared by HPH for 10 min (left) and 20 min (right).

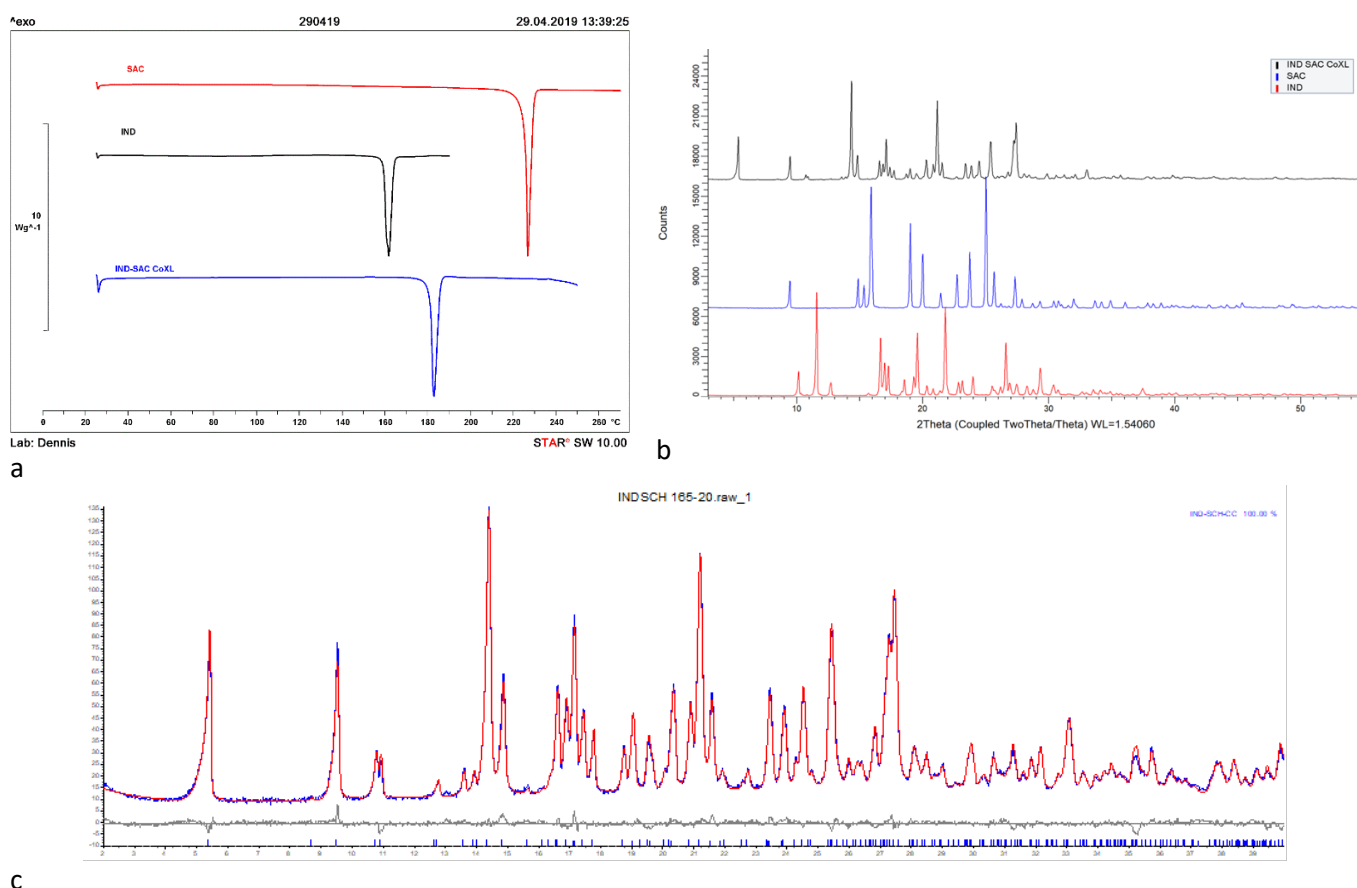


Fig. 6: a) DSC thermal profiles for bulk IND, SAC, and IND-SAC cocrystal, b) diffractograms of bulk materials and cocrystal prepared with different stabilisers by HPH, c) Rietveld refinement for the IND-SAC cocrystals presenting the measured pattern (blue line), the simulated pattern (red line) and the difference pattern (grey line).

R-Values: Rexp : 3.67 Rwp : 7.71 Rp : 5.58 GOF : 2.10 // Rexp` : 4.22 Rwp` : 8.86 Rp` : 6.56 DW : 0.57

Scanning electron microscopy was used to measure the crystal size obtained after the addition of stabilizers during homogenisation. The use of the water – soluble polymer Soluplus as a stabilizer led to the formation of

submicron range. All the crystals produced by HPH appeared of the same shape, where no deformation was also observed (**Fig. 7**).

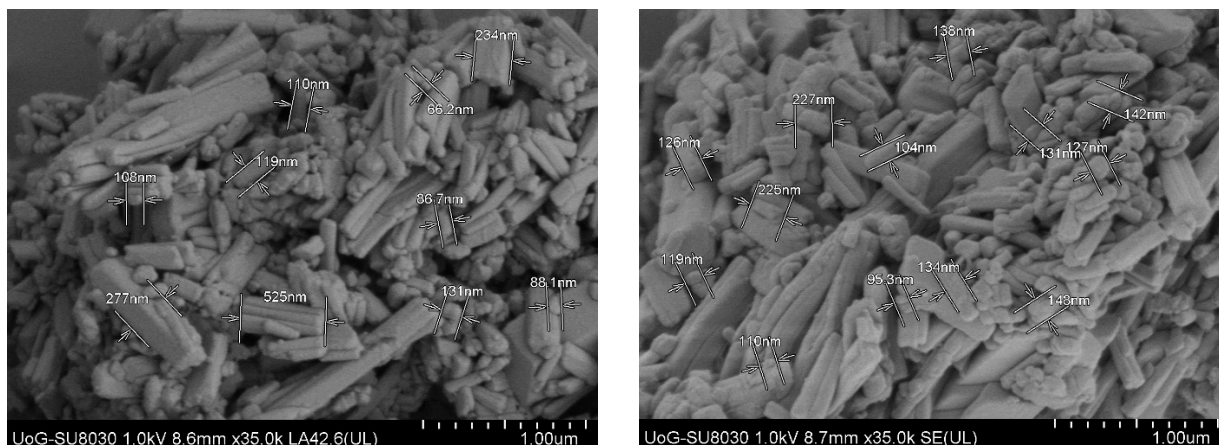


Fig. 7: SEM images of IND: SAC (1:1) cocrystals stabilised (Soluplus) with 0.5% w/v prepared by HPH.

Conclusions

The implementation of HPH as a processing technology for the synthesis of cocrystals and salts demonstrated that it can be effectively used and generate cocrystals in the micro and nanoscale. HPH is a robust process that can be easily scaled – up and produce high purity cocrystals co-processed with small polymer amounts that act as particle size stabilizers but also provide physical stability during storage.

Molecular modelling

All molecular modelling performed using Mercury CSD 3.7. CCDC-970189 (KTZ-OA) and CCDC-1501152 (CFX-MA) contain the crystallographic data for reference. The crystal structure of KTZ - OA can be seen in **Fig. 8A(left)** which shows a single ketoconazole and oxalic acid molecule in one asymmetric unit. This compound is classed as an oxalate salt because proton transfer takes place between the hydroxyl O-atom of the OA molecule and the imidazole N-atom of the KTZ molecule, resulting in then KTZ and OA moieties being bonded via a N (1)– H(1A)···O(4A) hydrogen bond. Strong Dimers are formed between the OA moieties via O(1A)–H(1AA)···O(3A) bidentate intermolecular hydrogen bonds. The imidazole ring of the KTZ molecule is linked to the contiguous OA dimers through a C–H···O hydrogen bond with the carbonyl O-atom of the OA moiety. The crystal packing arrangement of KTZ - OA salts can be seen in **Fig. 8B (left)**, showcasing the stacking interactions between KTZ's imidazole rings. The 5- and 6-member rings adopt an envelope and chair conformation respectively.

Thermal analysis by DSC

The thermal behaviour of the bulk materials, physical mixtures of them and prepared solid materials were investigated in the DSC, to monitor the effect of salification on the melting properties. It can be found that KTZ has a sharp melting point at 150.47 °C where OA displayed a melting point at 192°C (**Fig. 8a**). Three endothermic event occurred in the physical mixture of the API and the cofomer. The solid resulting from KTZ: OA (1:1.1) anti solvent process and atomization enhancement scCO₂ process showed a unique endothermic peak at approximately 194.77°C. There is no other endothermic event present in both materials, which indicates the formation of new crystal entity, different from the bulk materials. Comparing with the previously reported KTZ: OA salt data from *Martin et al.* (2013), KTZ OA (1:1.1) matches with the melting point of KTZ oxalate salt formed by solution crystallization method, confirming the formation of KTZ oxalate salt.

The solid resulting from the experiment, where scCO₂ was used as solvent, showed similar endothermic events like physical mixture of both compounds, which indicates the incomplete formation of salt and scCO₂ didn't solubilize the parent materials.

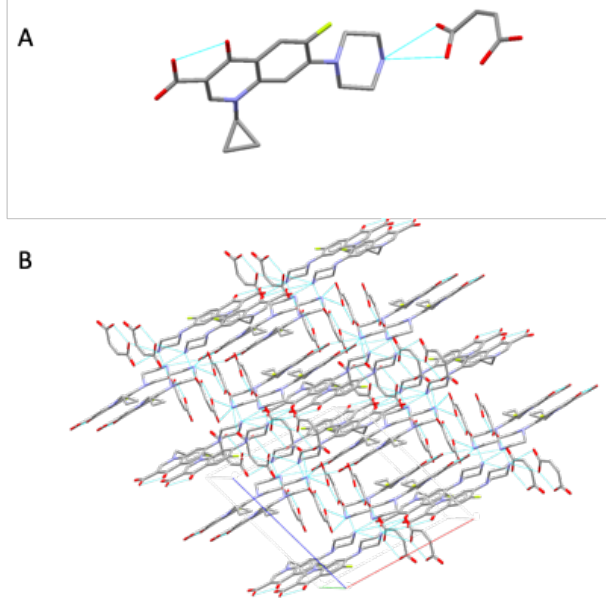
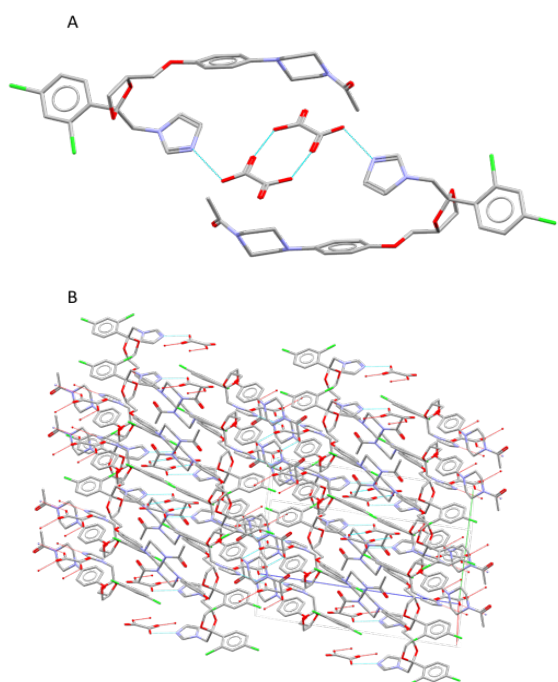
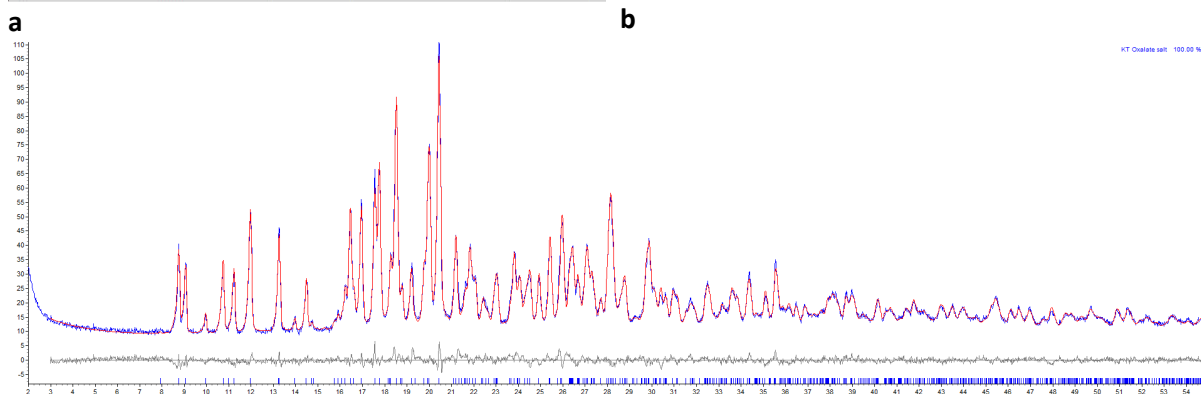
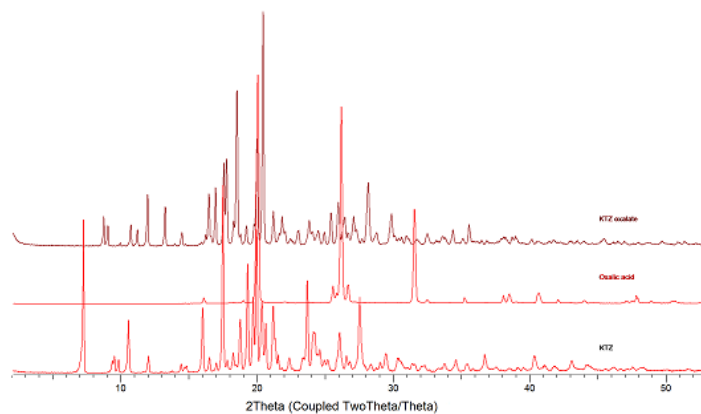
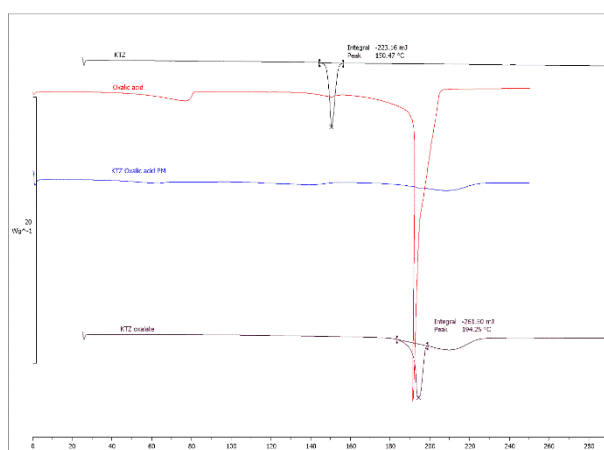


Fig. 8: Left:(A) Hydrogen bonds between OA dimers and imidazole ring of the KTZ moiety (B) Crystal packing projections for KTZ-OA salt. Other hydrogen and van der Waals bonds have been omitted for clarity. **Right:** A) Interaction between the CFX and MA molecules via dual N+ – HO hydrogen bonds (B) Crystal packing projections for CFX - MA salts. Other hydrogen and Van der Waals bonds have been omitted for clarity.



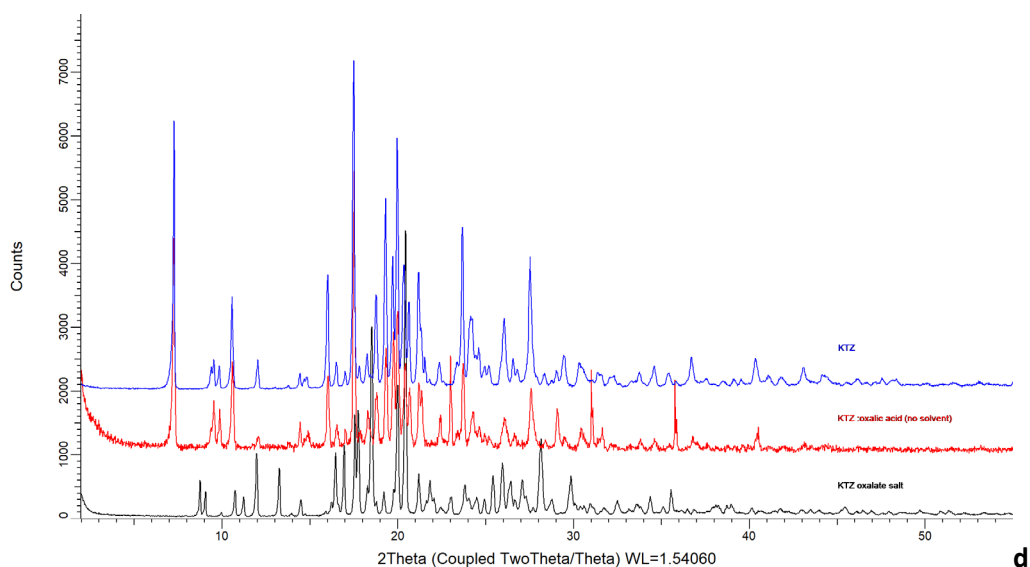


Fig. 9: a) DSC thermograms of bulk KTZ, OA, KTZ: OA PM and KTZ: oxalate salt prepared by SCF, b) PXRD pattern of bulk KTZ, OA and KTZ oxalate prepared by SCF processing, c) Rietveld refinement of the XRPD data for the TSE extruded KTZ: OA (1:1.1) representing the measured pattern (blue line), the simulated pattern (red line) and the difference pattern (greyline), d) PXRD pattern of bulk KTZ, KTZ: OA processed (with solvent and without solvent). **R-Values:** Rexp : 4.68 Rwp : 8.56 Rp : 6.59 GOF : 1.83 // Rexp` : 5.36 Rwp` : 9.82 Rp` : 7.81 DW : 0.76. Percentage match: KTZ: OA Salt: 100%

PXRD analysis

Bulk KTZ, OA and extruded KTZ: OA salt were further analysed by using PXRD to identify the crystal data obtained from each solid. Then this newly obtained data was compared with the previously reported data from the Cambridge structural database (CSD) by using TOPAS software. The percentage of the match between newly obtained crystal data with previously reported data is identified by Rietveld refinement of TOPAS V4.2 (Bruker). Though good fitting depends on visual fitting of the crystalline peak, but it is generally agreed that if the weighted profile R factor (Rwp) is within or around 3 times of the expected R factor (Rexp), the match or refinement is satisfactory¹⁴. The main intense peaks for KTZ appear at 7.28°, 9.5°, 10.69°, 11.96°, 16.13°, 17.5°, 20.01° and 27.65° 2θ. Some other small peaks were also found. The coformer, OA, showed diffraction peaks at 16.09°, 19.03°, 20.11°, 26.24°, and 31.57° 2θ (**Fig.9b**). As observed, a distinct crystalline profile was obtained for the KTZ OA SCFs processed solid materials at 8.75°, 10.81°, 11.95°, 13.27°, 17.72°, 18.5°, 19.89°, 20.42°, and 28.14° 2θ which doesn't match with the bulk KTZ and OA crystal data that confirms the formation of a new solid crystal. Furthermore the diffractogram for the KTZ: OA salts produced in this study compared with the previously generated data, by *Martin et al* taken from the CSD. After fitting the structural data of the salts obtained in this experiment to those taken from the CSD, it was found that both the anti-solvent and atomization produced salts had a 100% match with the reference data. This indicates that the salts produced in this study have 100% purity, with no unreacted substances or contaminants present, confirming Atomization and Anti-solvent scCO₂ processing as a valid technique for salification (**Fig.9c**).

In the case of solvent assisted scCO₂ processing, where, where scCO₂ was used as solvent the diffraction peaks do not closely match with the salt standard or the salts formed through anti-solvent and atomization methods. Here, the produced substance more closely resembles bulk KTZ, indicating that solvent based methods are not suitable for salification in this instance (**Fig. 8d**).

Morphological study

Only promising candidate samples were further analysed by SEM to find the morphological properties of the KTZ oxalate salt prepared by SCFs processing. The images shown in **Fig. 9** show marked morphological differences between the bulk material and produced salt.

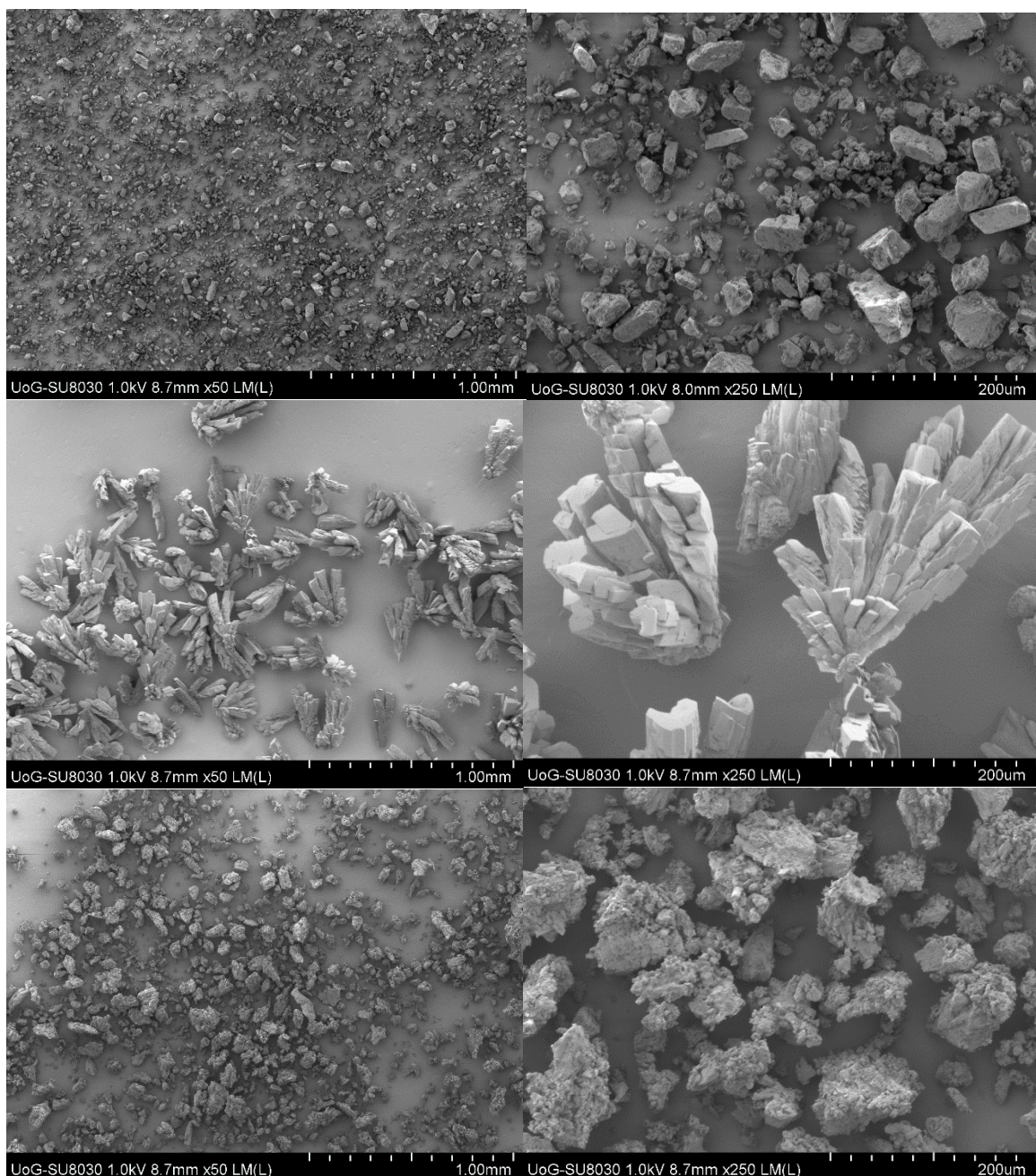


Fig. 9: SEM images of KTZ bulk (top –left and right), KTZ oxalate formed by antisolvent (middle- left and right) and atomization enhancement (bottom - left and right) by scCO₂ processing.

Bulk KTZ looks crystalline with small and large crystals packed together but not of a unique shape. KTZ:OA salts prepared by antisolvent SCFs show a block and needle crystalline shape, although KTZ oxalate formed by SCFs atomization enhancement, consists of an agglomeration of crystals full with block shaped single crystals.

Fourier transform infrared spectroscopy

FT-IR spectra of bulk KTZ, OA, KTZ: OA PM and salt obtained by SCFs processing were obtained to evaluate the possible interaction between KTZ and OA. The comparison of the IR spectra of bulk materials with synthesized salt was studied to validate the proton transfer between the salt former and the API. KTZ showed characteristic broad NH-stretch peak¹⁵ at 3125 cm⁻¹. The peak at 1644 and 1370 cm⁻¹ was observed due to carbonyl C=O stretch¹⁷ and C=C of aromatic ring of KTZ (**Fig. 10a**).

The organic compound of OA has two carboxylic acid COOH groups. The -C(=O)OH group is characterized by the OH stretch, the C=O stretch, C-O stretch, OH in-plane deformation and the OH out-of-plane deformation modes. An O-H group of OA is present in the region of 3100-2500 cm^{-1} due to presence of dihydrate water in the molecule, whilst the intense peak at 1695 cm^{-1} due to C=O stretching. In the present study, C=O stretching mode is attributed at 1678 cm^{-1} (weak) in OA and the C-O stretching of carboxylic acid is identified at 1150 cm^{-1} in the IR spectrum of both compounds ¹⁶.

In the KTZ-OA salt, the C=O group stretching of KTZ shift to 1622, whilst a new peak observed at 1746 cm^{-1} . The presence of shifting in the vibrational frequencies of KTZ and OA indicates the formation of a Supramolecular heterosynthron in the multicomponent salt. The loss of a broad band OH group of water molecules in OA dihydrate after the formation of salt can show the absence of water in KTZ OA salt crystals ¹⁸.

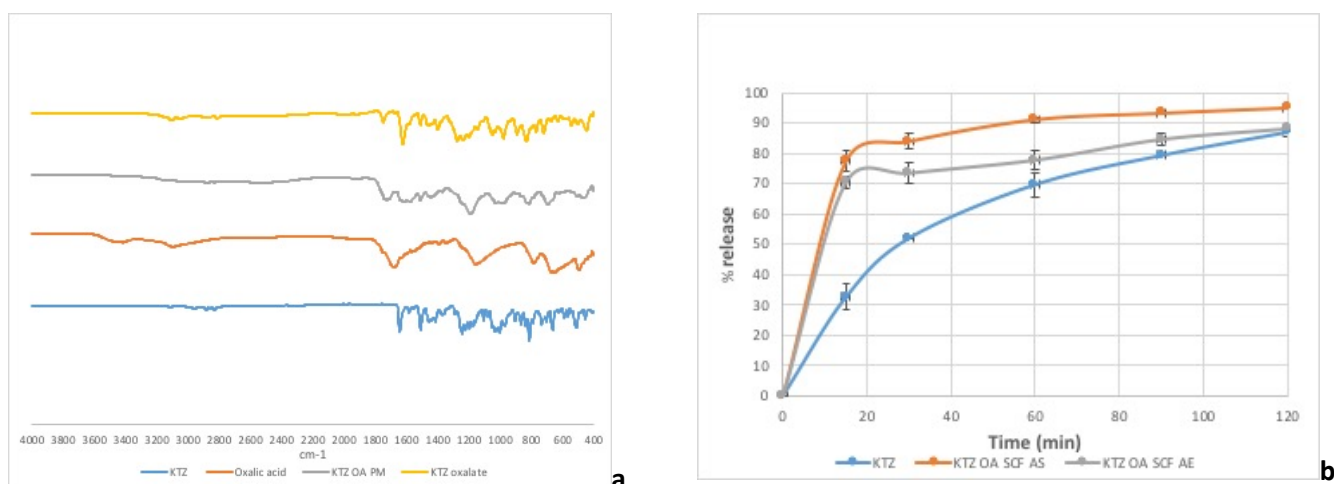


Fig. 10: a) FTIR spectroscopic analysis of bulk materials and KTZ OA salt, b) Release profile of bulk KTZ and SCF processed KTZ oxalate salt.

Dissolution study

The dissolution profiles of KTZ and KTZ: OA salts prepared by antisolvent and atomization enhancement by SCF processing are shown in Fig. 8, and the % release of prepared salt was compared with bulk KTZ to compare the difference between them. As KTZ is a low water-soluble drug it showed very slow increase of drug release compared to KTZ: OA salt. After 15 minutes KTZ showed only 34% release of drug whereas in the same time period KTZ oxalate salt showed more than 70% release for salts prepared through atomization SCF and 78% for salts processed using anti-solvent SCF (**Fig.10b**). In the one-hour release profile KTZ oxalate salt showed about 90% release compared to 70% release of bulk KTZ. After two hours of dissolution time, the KTZ bulk release catches up with the KTZ:OA salts prepared through atomization, though the anti-solvent prepared solutions still demonstrates superior solution with 96% drug release.

Conclusions

This research highlights how scCO_2 processing is a valid method of salt production, with both Anti-solvent and Atomization SCF methods achieving high-grade pharmaceutical salts which demonstrate 100% purity. The KTZ: OA salts demonstrate far more rapid dissolution compared to the bulk KTZ, indicating they have improved solubility. Interestingly, while the salts produced both show a 100% match with the reference crystal, it seems that you can achieve different crystal forms of the KTZ: OA salts depending on which SCF method you use, with SEM data showing a marked morphological difference between the atomization and anti-solvent prepared salts, and with there being different dissolution properties between the salts. These methods of SCF offer a more environmentally friendly, solvent free alternative to classic salification methods.

References

1. Chadha, R., Singh, P., Khullar, S., & Mandal, S. K. (2016). *Crystal Growth and Design*, 16(9), 4960–4967
2. Serajuddin, A. T. M. (2007). Salt formation to improve drug solubility. *Advanced Drug Delivery Reviews*, 59(7), 603–616
3. Martin, F., Pop, M., Borodi, G., Filip, X. & Kacso, I. (2013). *Crystal Growth & Design*, 13(10), 4295-4304
4. Almeida E Sousa, L., Reutzel-Edens, S. M., Stephenson, G. A., & Taylor, L. S. (2016). *Crystal Growth and Design*, 16(2), 737–748.
5. Savjani, K. T., Gajjar, A. K., & Savjani, J. K. (2012). *ISRN Pharmaceutics*
6. Elder, D. P., Holm, R., & De Diego, H. L. (2013). *International Journal of Pharmaceutics*, 453(1), 88–100
7. Malamataris, M., Ross, S. A., Douroumis, D., & Velaga, S. P. (2017). *Advanced Drug Delivery Reviews*.
8. Rodrigues, M., Velaga, S., & Fernandes, A. C. (n.d.). Supercritical Fluids As Alternative Media for the, (778168).
9. Trivedi, V., Bhomia, R., Mitchell, J. C., Coleman, N. J., Douroumis, D., & Snowden, M. J. (2013). Study of the effect of pressure on melting behavior of saturated fatty acids in liquid or supercritical carbon dioxide. *Journal of Chemical and Engineering Data*, 58(6), 1861–1866.
10. Padrela, L., Rodrigues, M. A., Velaga, S. P., Matos, H. A., & de Azevedo, E. G. (2009). Formation of indomethacin-saccharin cocrystals using supercritical fluid technology. *European Journal of Pharmaceutical Sciences*, 38(1), 9–17.
11. <http://www.foodtech-portal.eu/index.php?title=Special:PdfPrint&page=High+pressure+homogenisation>
12. http://cdn2.hubspot.net/hub/231301/file-20766082-pdf/docs/micro_debee.pdf
13. Fernández-Ronco, M. P., Kluge, J., & Mazzotti, M. (2013). High-pressure homogenization as a novel approach for the preparation of co-crystals. *Crystal Growth and Design*, 13(5), 2013–2024.
14. Toby, B. H. (2006). R factors in Rietveld analysis: How good is good enough? *Powder Diffraction*, 21(1), 67–70.
15. Shayanfar, A., & Jouyban, A. (2014). Physicochemical characterization of a new cocrystal of ketoconazole. *Powder Technology*, 262, 242–248.
16. Kamble, R. N., Bothiraja, C., Mehta, P. P., & Varghese, V. (2018). Synthesis, solid state characterization and antifungal activity of ketoconazole cocrystals. *Journal of Pharmaceutical Investigation*, 48(5), 541–549.
17. Muthuselvi, C., Arunkumar, A., & Rajaperumal, G. (2016). Growth and Characterization of Oxalic Acid Doped with Tryptophan Crystal for Antimicrobial Activity. *Der Chemica Sinica*, 7(4), 55–62.
18. Alatas, F., Ratih, H., & Soewandhi, S. N. (2015). Enhancement of solubility and dissolution rate of telmisartan by telmisartan-oxalic acid co-crystal formation. *International Journal of Pharmacy and Pharmaceutical Sciences*, 7(3), 423–426.

B) Design of 4 novel pharmaceutical cocrystal compounds with improved stability and dissolution rates using various techniques

1) Product#1: Perampanel -Saccharin cocrystal

Preparation methods:

Hot-melt extrusion- A homogeneous physical mixture was prepared through accurately weighing bulk components in stoichiometric ratio (1:1) and then blending in a Turbula TF2 mixer (Willy A. Bachofen AG, Switzerland) at 100 rpm for 10 min. The blend was then placed in a twin-screw volumetric feeder before being fed into a 10mm twin-screw extruder (Rondol, France) at 0.8 g/min. A maximum temperature of 125 °C was used and a screw-speed of 20rpm.

Ball Milling- A 1:1 stoichiometric ratio of the physical blend prepared by Turbula was placed in a Mixer Mill MM 400 (Retsch, Germany) which was used to grind the cocrystal materials. The materials were loaded into a 25 ml metal grinding jar, with a steel grinding ball at room temperature. The vibrational frequency was set to 30 Hz and with the successful cocrystal milled for 6 minutes under these conditions.

High-Pressure Homogenization- A 1:1 stoichiometric physical blend was dissolved in a 50 ml solvent mixture of acetonitrile and acetone (1:1). After being fully dissolved, the solution was transferred and homogenized in a Micro Debee laboratory homogeniser (South Easton, MA, USA) at 15000 psi for a predetermined time at room temperature. At the end of the homogenization process, the solid was separated by filtration under vacuum. The filtrate was dried overnight at 50°C and stored for further analysis.

Analysis:

Computational analysis

Perampanel (PER) has an accessible molecular geometry containing 3 off-shooting aromatic rings all containing easily accessible acceptor sites as well as two major donor sites at N3 and O1, so dimer formation will be preferred and is small and flexible, making it a friendly molecule to work with. Saccharin (SACC) scored highly during hydrogen bond propensity and molecular complementarity screening, indicating that the two compounds have a complimentary geometry and have a strong disposition to forming hydrogen bonds. SACC contains a strong hydrogen bond acceptor (C=O) and strong donors (N-H) to form a robust imide homodimer synthon in the crystal structure.

Thermal Analysis

Thermal analysis via DSC revealed that bulk PER melting onset begins at 174.40 °C, while SACC is known to display a sharp melting peak at 229.47 °C¹. The physical mixture of the two components displayed a single broad melting endotherm at 149.38 C. Analysis of the produced suspected PER-SACC cocrystal revealed a single sharp melting point at 143.83 °C, with the absence of any event occurring at the melt points of the bulk components, indicating that the material is of a new crystal form². Though it typical for physical mixtures to display a eutectic point of cocrystal forming, followed by the cocrystal melt, it should be noted that as the melt point of the cocrystal is actually lower than the two bulk components, this will not be the case as the cocrystal has already formed and melted before reaching this point. Though this is uncommon, it demonstrates high reactivity between the PER and SACC. This is likely due to the complementary bonding sites along the aromatic rings of the PER molecule and the N-H donors of SACC allowing for robust dimer formation, without the need to heat the molecules to higher temperatures along the extruder barrel. It is possible that the high-shear mixing provided enough energy for dimer formation along the barrel, while in the ball milling experiment this would have been allowed through the intense kneading brought on by the high vibrational frequency.

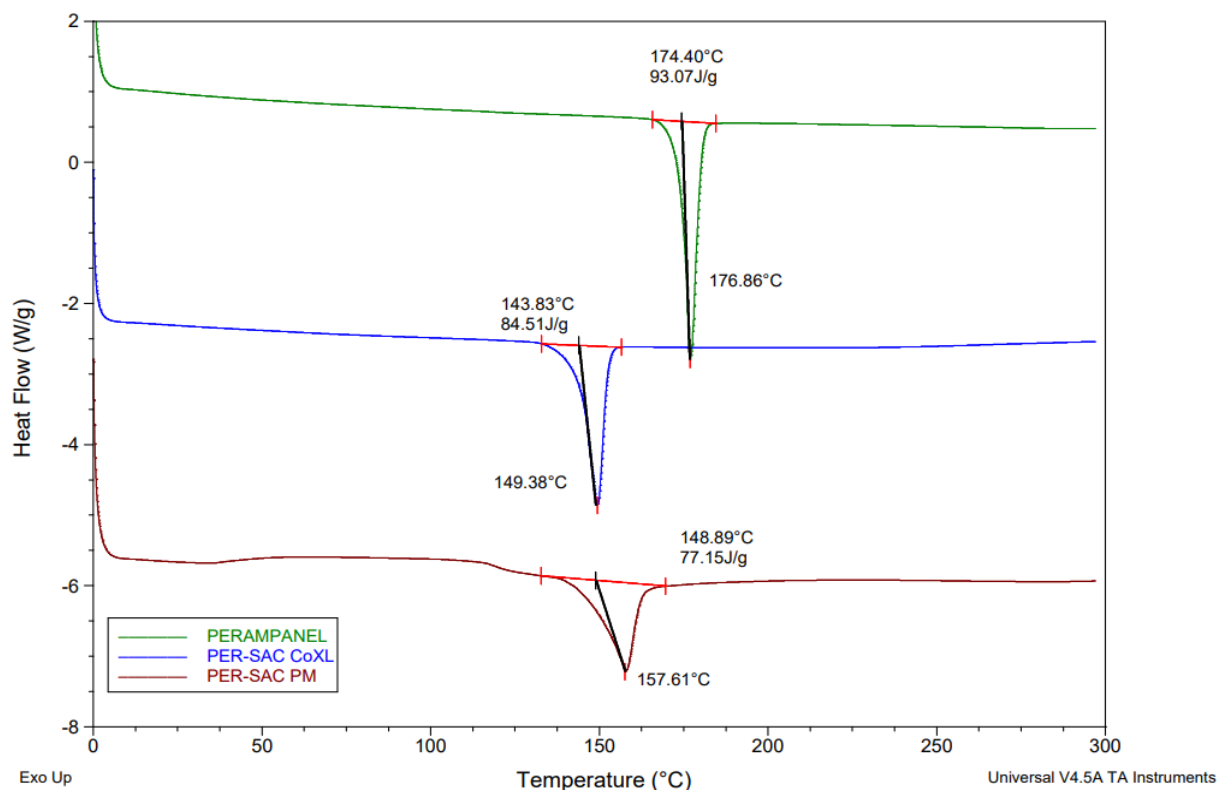


Figure 1: Thermograms of bulk RIVA, RIVA-SACC PM and RIVA-SACC cocrystal.

X-Ray analysis:

Bulk materials, physical mixture and the cocrystals were further analysed via X-ray diffraction, where PER displayed characteristic peaks at 4.71, 7.83, 9.38, 10.25, 14.06, 15.14 and 16.04 °2θ. SACC displayed intensity peaks at 9.56, 15.91, 16.02, 17.23, 19.13, and 25.14 °2θ and the physical mixture containing a mix of these angular points. The PER-SACC cocrystal displayed a unique crystal diffraction pattern, independent of the two bulk components indicating the presence of a new crystal form. The PER-SACC cocrystal displayed new peaks at 7.46, 8.21, 10.79, 11.87, 12.23, 15.51 °2θ, as well as a new cluster of peaks between 21-22 °2θ. These results, in combination with the DSC analysis reveal that we are working with a new cocrystal structure.

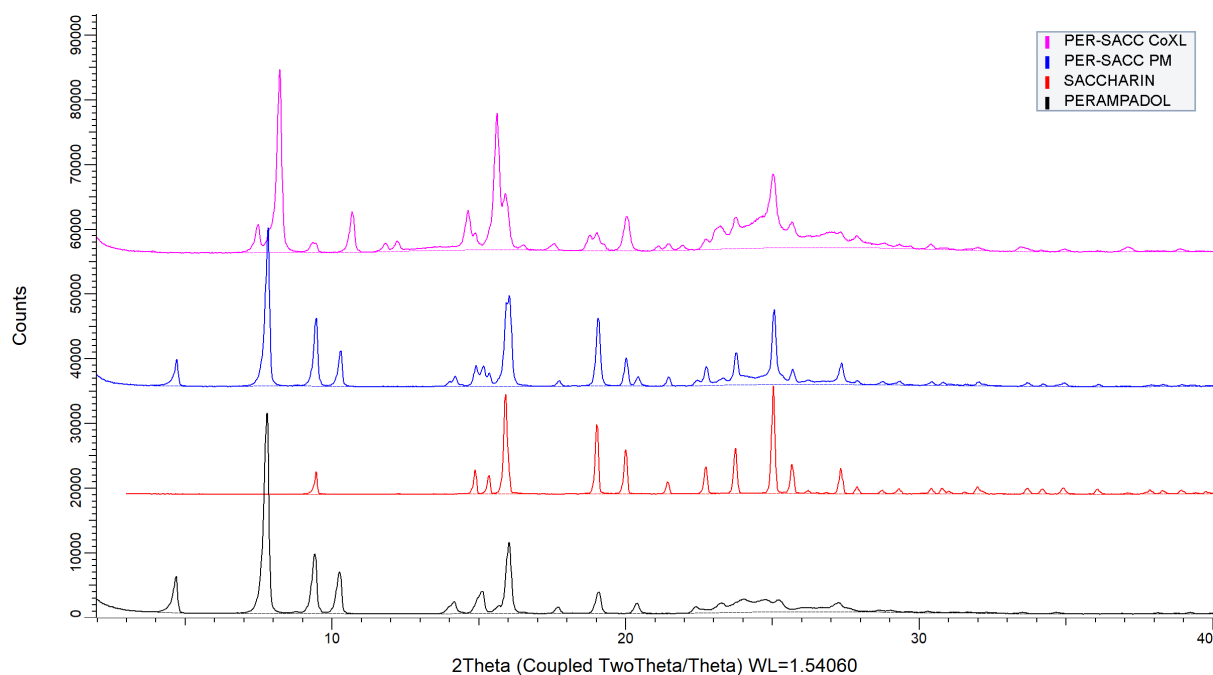
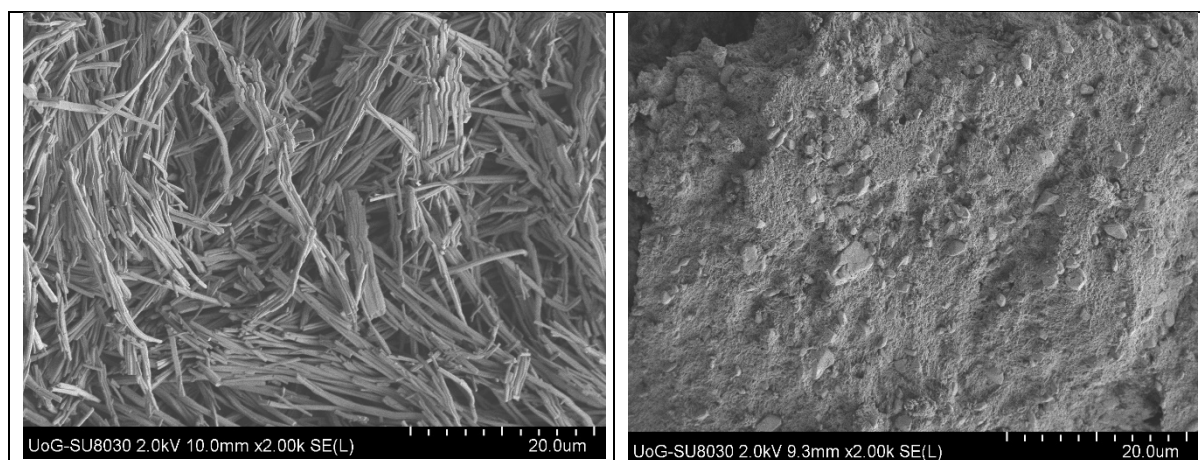


Figure 2: Diffraction pattern of bulk PER, bulk SACC, PER-SACC PM and PER-SACC cocrystal.

Scanning Electron Microscopy:

SEM analysis revealed a pronounced difference in the morphology and particle size of the PER-SACC Cocrystal compared to the bulk constituents. The bulk PER particles are long, slender, fibrous prisms arranged in a disordered fillform like arrangement, roughly 30-10um in length. The bulk SACC particles are made up of both a rod-shaped and sub-rounded oblate morphology, mostly greater than 20um in size. The PER-SACC cocrystals have a much smaller particle size, with the rod-like particle measuring less than 1.0um, compared to the longer, slenderer active. Interspersed among these are a number of rounded, equant particles, measuring around 2-5um in size.



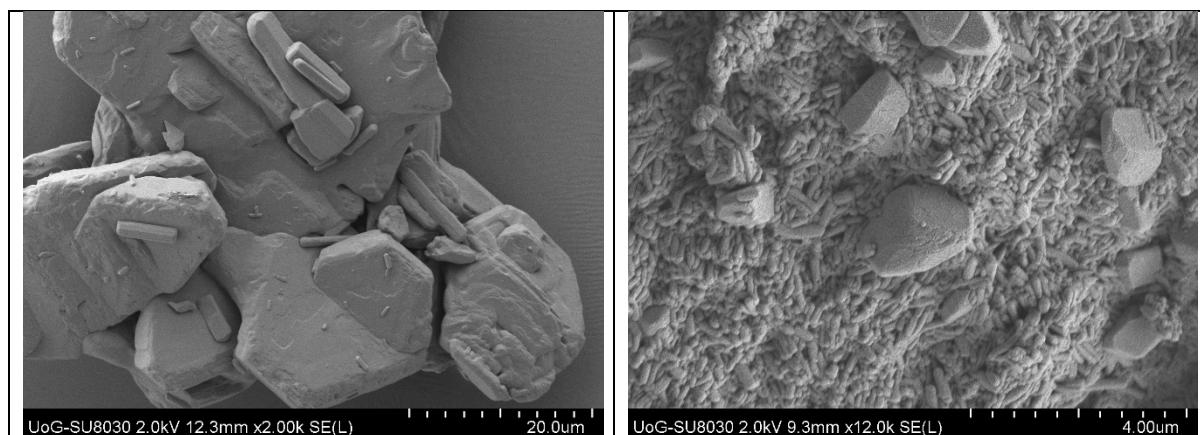


Figure 3: Images Bulk PER (top left), Bulk SACC (bottom left) and PER-SACC Cocrystal from two different magnifications (right)/

2) Product#2: Apixaban - Oxalic Acid cocrystal

Preparation methods:

Hot-melt extrusion- A homogeneous physical mixture was prepared through accurately weighing bulk components in stoichiometric ratio (1:1) and then blending in a Turbula TF2 mixer (Willy A. Bachofen AG, Switzerland) at 100 rpm for 10 min. The blend was then placed in a twin-screw volumetric feeder before being fed into a 10mm twin-screw extruder (Rondol, France) at 1.0 g/min. A maximum temperature of 190 °C was used and a screw-speed of 12 rpm.

Ball Milling- A 1:1 stoichiometric ratio of the physical blend prepared by Turbula was placed in a Mixer Mill MM 400 (Retsch, Germany) which was used to grind the cocrystal materials. The materials were loaded into a 25 ml metal grinding jar, with a steel grinding ball at room temperature. The vibrational frequency was set to 30 Hz and with the successful cocrystal milled for 10 minutes under these conditions.

High-Pressure Homogenization- A 1:1 stoichiometric physical blend was dissolved in a 50 ml solvent mixture of Acetic acid and ethanol (50:50). After being fully dissolved, the solution was transferred and homogenized in a Micro Debee laboratory homogeniser (South Easton, MA, USA) at 15000 psi for a predetermined time at room temperature. At the end of the homogenization process, the solid was separated by filtration under vacuum. The filtrate was dried overnight at 50°C and stored for further analysis.

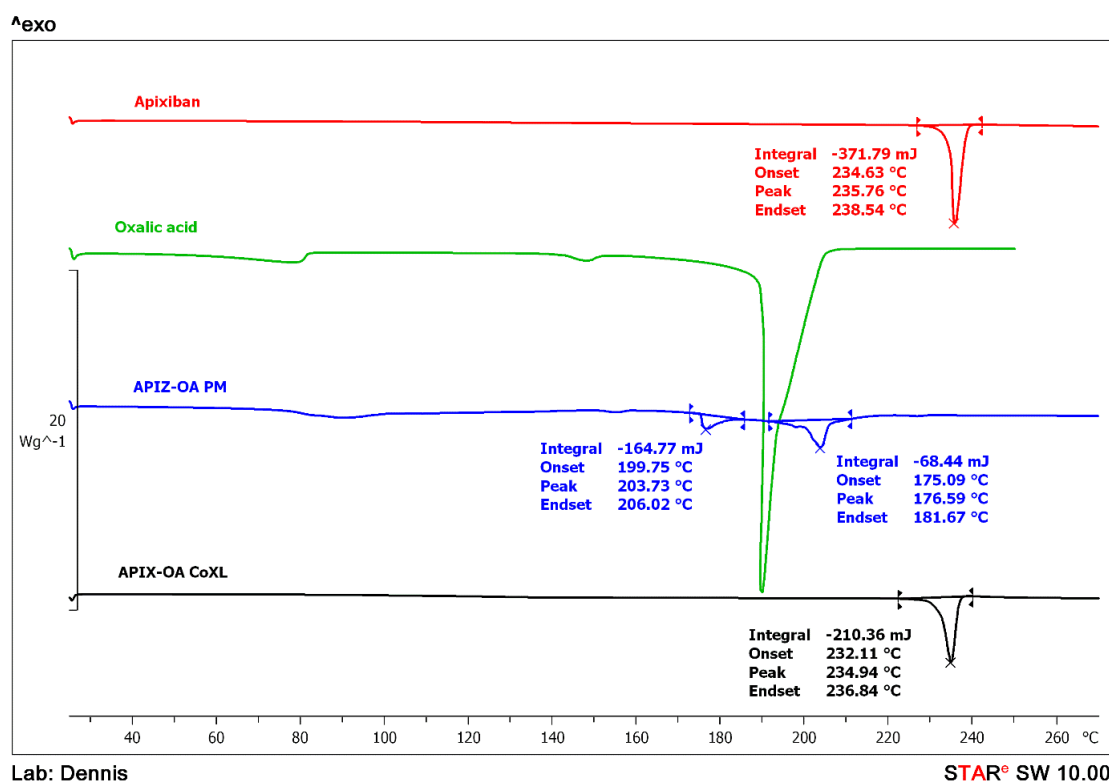
Analysis:

Computational analysis

Apixaban (APIX) observed to have a plethora of easily assessable donor and acceptor sites, with easily accessible geometries, robust dimer forming abilities and has a tendency to bond with molecules with a negative molecular surface. Has two excellent Donor sites at O1 and O3. Complementarity analysis further demonstrated this drug's ability to form hydrogen bonds with a variety of coformers containing carboxylic and hydroxyl groups. Oxalic Acid (OA) has demonstrated robust dimer forming ability with complementary OA groups. Strong possibility of APIX forming dimers through a C–H...O hydrogen bond with the carbonyl O-atom of the OA moiety

Thermal analysis:

Bulk APIX displays melting onset of 234.63 °C, while the OA coformer shows a large melting endotherm at 189.92 °C. The physical mixture displays the initial eutectic melt at 175.09 °C followed by a second melt at 199.75 °C. This is likely a depressed cocrystal melt, due to the presence of impurities. This is further supported by the broad onset of the melt, suggesting the cocrystal formed within the DSC instrument was not a pure cocrystal, and contained remaining impurities from parent compounds⁴. For this reason, a slow screw speed was selected during extrusion, to enhance the possibility of cocrystallization occurring across the barrel. The APIX-OA cocrystal displays a single melt between the melts of its two parent compounds at 232.11 °C. The Single melting endotherm for the APIX-OA sample indicates a pure substance, with the absence of any impurity or bulk constituent². Though



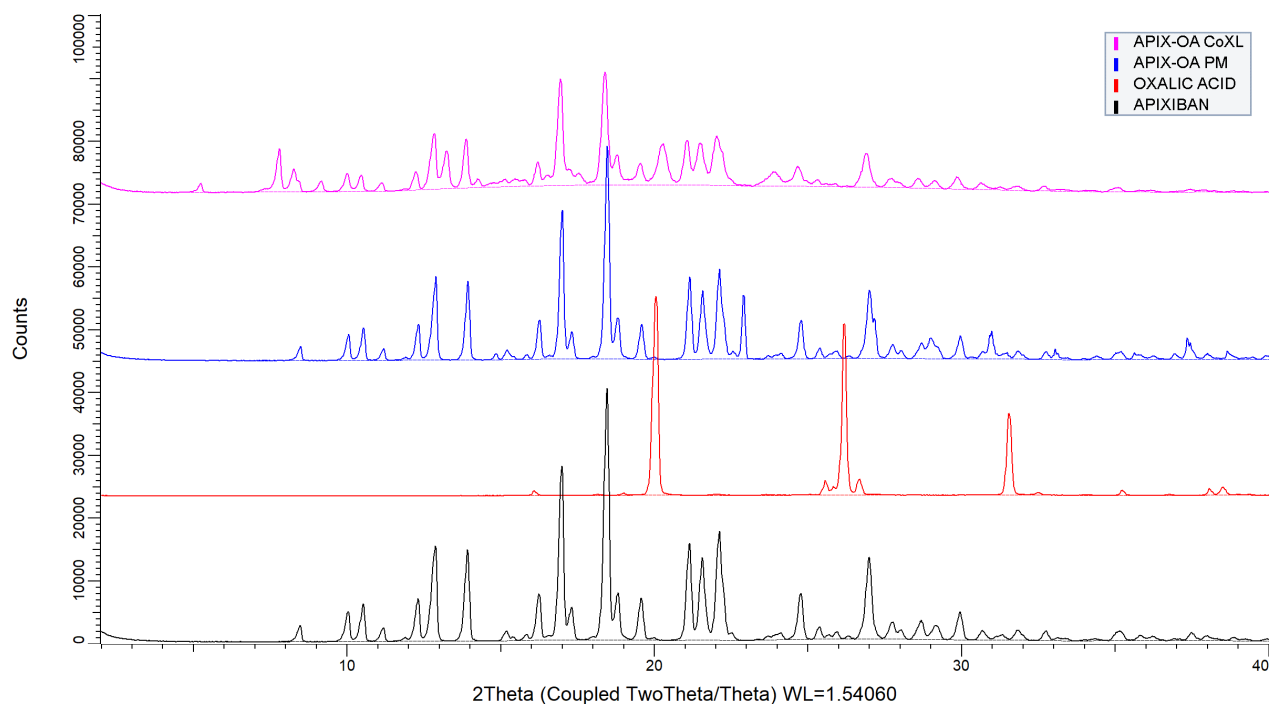
Lab: Dennis

STAR[®] SW 10.00

Figure 1: Thermograms of bulk APIX and OA, APIX-OA PM and APIX OA cocrystal.

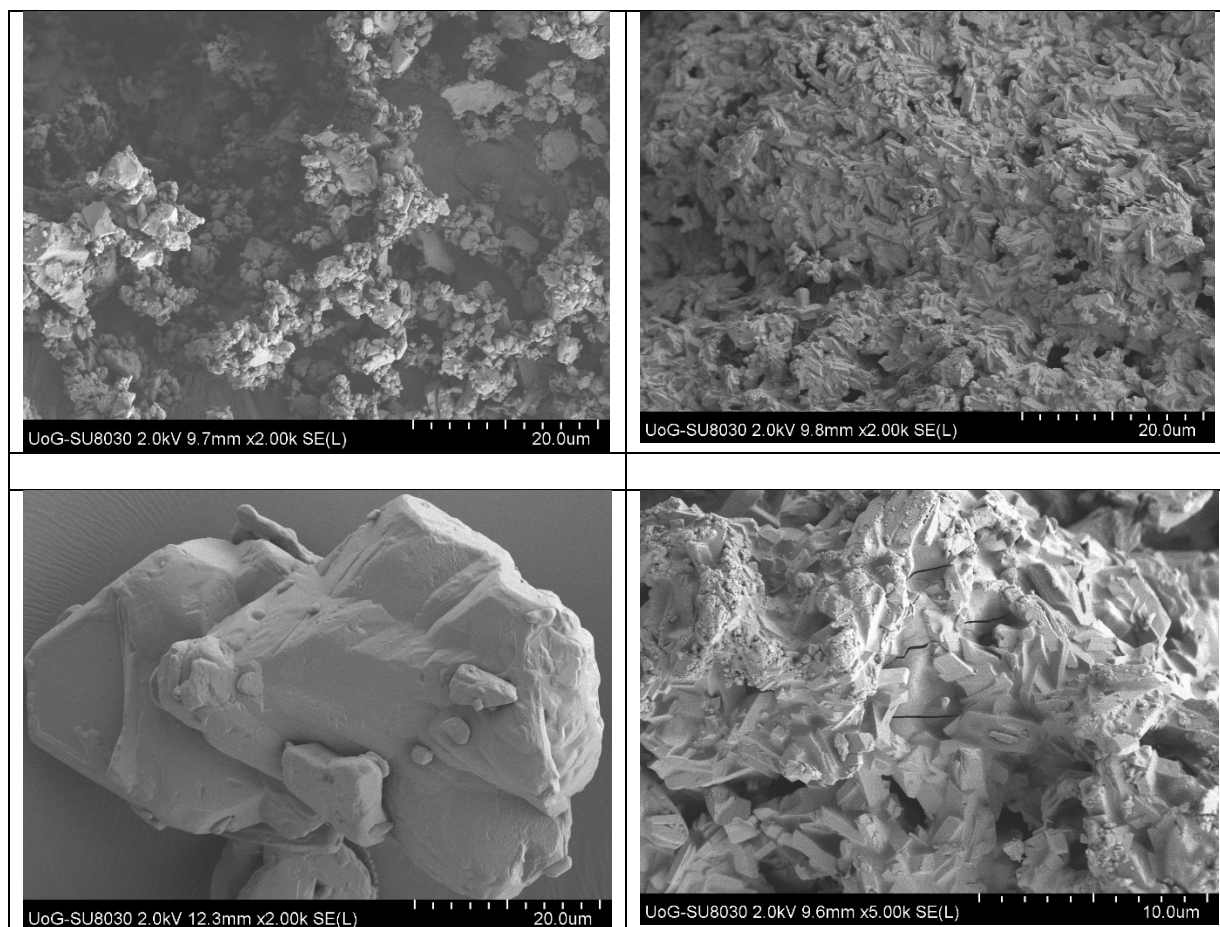
X-Ray Analysis:

Bulk APIX displays characteristic diffraction peaks at 8.41, 12.83, 13.87, 17.02, 18.46, 22.14 and 27.04 °2θ. Oxalic acid has three characteristic peaks at 20.06, 26.17 and 31.58°2θ. The unique diffractogram seen for the APIX-OA cocrystal shows new, novel peaks at 5.28, 7.84, 8.27, 9.71, 16.72, and 20.23 °2θ. This diffractogram was screened against documented CCDC samples using EVA phase analysis software and TOPAS, which no close matches being found.



Scanning Electron Microscopy:

SEM analysis showed notable, morphological differences between the bulk constituents compared the cocrystal sample. Bulk APIX showed a network of irregular shaped, equant particles stacked in a capillary-like network. This is likely due to the static nature of the APIX powder. The bulk SACC particles analysed here display an Oblate/tabular morphology, with a relatively high particle size compared to the API and cocrystal (50um >). The APIX-SACC cocrystals however, appear elongated, with a can be seen to be made up of rod-like, tabular particles morphology. It can be seen that the individual APIX-SACC particles have agglomerated to form a inter-connected matrix around groups of particles. Many of the individual particles appear to be irregular in shape, with no consistent particle size, though this is difficult to ascertain, due to the presence of the matrix network. No individual particle appears to be over 5.0um however, showing limited particle size reduction due to the mechanochemical grinding process'.



References

1. Basavoju S, Boström D, Velaga S. Indomethacin–Saccharin Cocrystal: Design, Synthesis and Preliminary Pharmaceutical Characterization. *Pharmaceutical Research*. 2007;25(3):530-541.
2. Ross S, Lamprou D, Douroumis D. Engineering and manufacturing of pharmaceutical co-crystals: a review of solvent-free manufacturing technologies. *Chemical Communications*. 2016;52(57):8772-8786.
3. Chadha K, Karan M, Bhalla Y, Chadha R, Khullar S, Mandal S et al. Cocrystals of Hesperetin: Structural, Pharmacokinetic, and Pharmacodynamic Evaluation. *Crystal Growth & Design*. 2017;17(5):2386-2405.
4. Saganowska P, Wesolowski M. DSC as a screening tool for rapid co-crystal detection in binary mixtures of benzodiazepines with co-formers. *Journal of Thermal Analysis and Calorimetry*. 2017;133(1):785-795.

3) Product#3 : Rivaroxaban-Hesperitin Cocrystal

Preparation methods:

Hot-melt extrusion- A homogeneous physical mixture was prepared through accurately weighing bulk components in stoichiometric ratio (1:1) and then blending in a Turbula TF2 mixer (Willy A. Bachofen AG, Switzerland) at 100 rpm for 10 min. The blend was then placed in a twin-screw volumetric feeder before being fed into a 10mm twin-screw extruder (Rondol, France) at 0.8 g/min. A maximum temperature of 180 °C was used and a screw-speed of 15rpm.

Ball Milling- A 1:1 stoichiometric ratio of the physical blend prepared by Turbula was placed in a Mixer Mill MM 400 (Retsch, Germany) which was used to grind the cocrystal materials. The materials were loaded into a 25 ml metal

grinding jar, with a steel grinding ball at room temperature. The vibrational frequency was set to 30 Hz and with the successful cocrystal milled for 10 minutes under these conditions.

High-Pressure Homogenization- A 1:1 stoichiometric physical blend was dissolved in a 50 ml solvent mixture of acetonitrile and DMSO (9:1). After being fully dissolved, the solution was transferred and homogenized in a Micro Debee laboratory homogeniser (South Easton, MA, USA) at 15000 psi for a predetermined time at room temperature. At the end of the homogenization process, the solid was separated by filtration under vacuum. The filtrate was dried overnight at 50°C and stored for further analysis.

Analysis:

Computational analysis

Analysis revealed Rivaroxaban (RIVA) has many easily accessible donor sites, so cofomers with a large number of acceptor sites would work well. In addition to this there is a strong and easily accessible acceptor sites around the CL1 ring. This was advantageous as hesperitin (HESP) has a high donor count and showed high bonding propensity, and dimer forming ability between OH sites and RIVA CL 1 ring.

Thermal Analysis:

Bulk RIVA displays sharp melting endotherm at 231.26 °C, while HESP is known to melt at 231.71 °C³. The physical mixture shows a broad, multi-event melt at 186.17 °C. The RIVA-HESP cocrystals melt lies at 207.33 °C, displaying a sharp melt, suggesting high purity. That the thermal profile for the cocrystal displays a single melting endotherm, with the absence of any base material suggests the formation of a new crystal form. A physical mixture of a cocrystal constituents will often display the eutectic melt, followed by a small recrystallization event and the cocrystal melt, though as the eutectic melt and cocrystal melting point are relatively close together it seems that this all occurred during the single broad melt. This would explain why the melt seems to contain multiple events. There is a small endothermic event around 197.2 °C which could be related to the recrystallization followed by another endothermic event at 207.91 °C, which would correspond with the melting point of the cocrystal form.

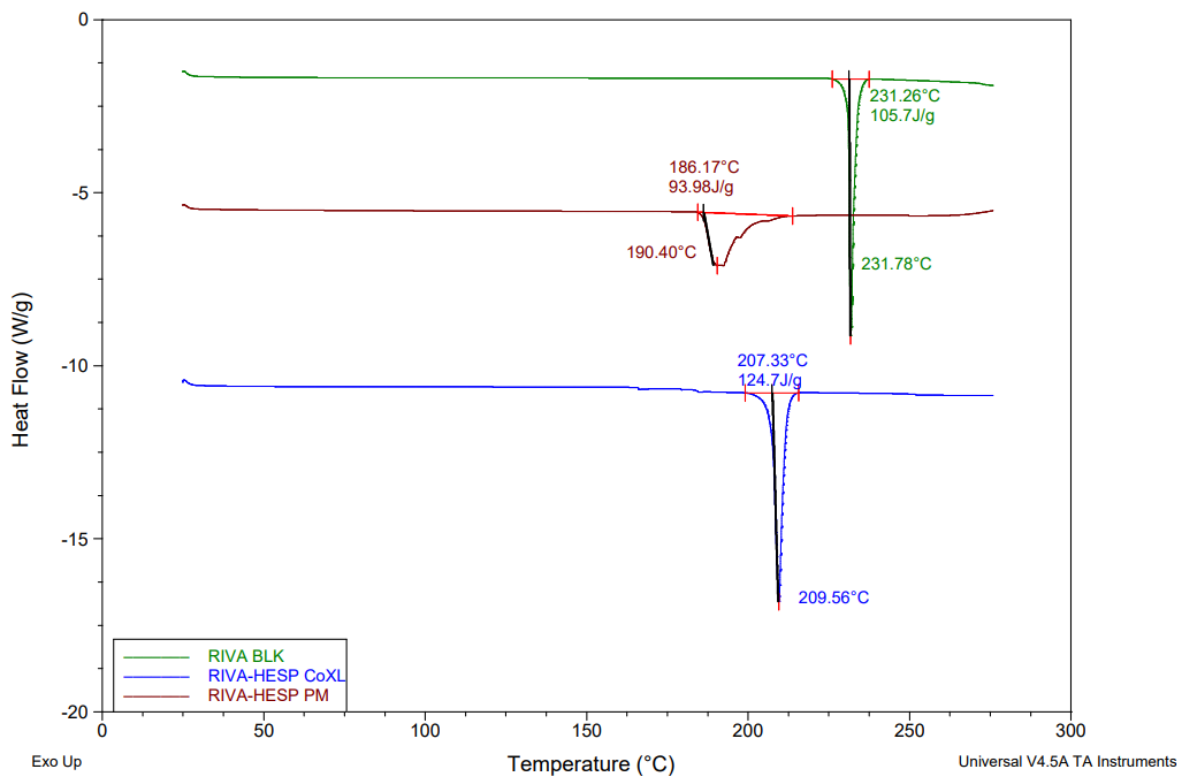


Figure 1: Thermograms of bulk RIVA, RIVA-SACC PM and RIVA-SACC cocrystal.

X-Ray analysis:

Bulk materials, physical mixture and the cocrystals were further analysed via X-ray diffraction. Bulk RIVA displayed characteristic peaks at 9.02, 14.33, 16.55, 19.58, 19.96, 22.54 and 26.68 °2θ. HESP displayed intensity peaks at 7.23, 14.59, 17.02, 17.73, 26.26, and 29.55 °2θ and the physical mixture containing a mix of these angular points. The RIVA-HESP CoXL displayed a unique diffraction pattern, fitting to no submitted structures found in the Cambridge structural database (CCDC), with a number of unique intensity peaks, not seen in either bulk constituent. The intensity peaks seen at 8.39, 9.51, 11.92, 18.89, 21.29 and 25.64 suggest the formation of a new, crystalline cocrystal form of RIVA.

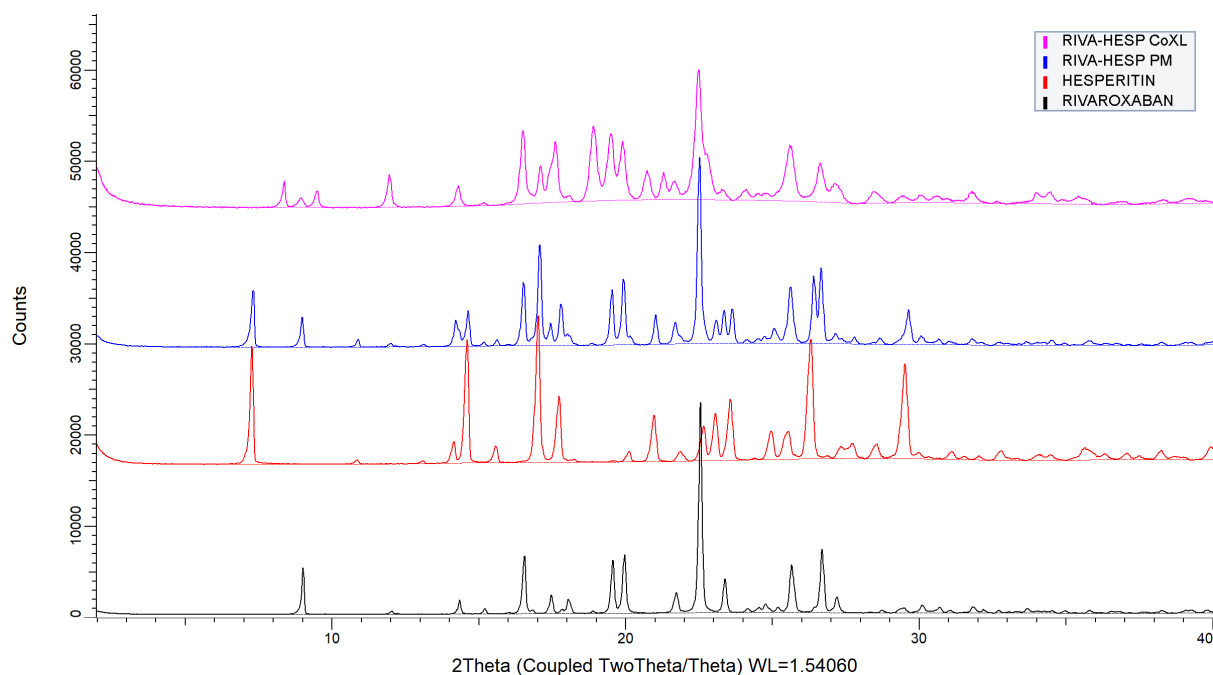
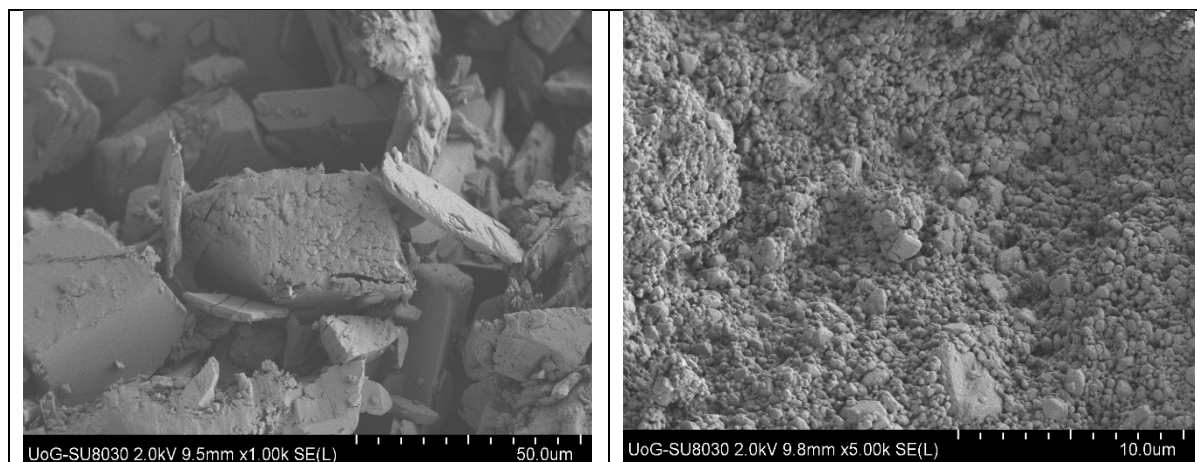


Figure 2: Diffraction pattern of bulk RIVA, bulk HESP, RIVA-HESP PM and RIVA-HESP cocrystal.

Scanning Electron Microscopy:

SEM analysis revealed vast differences in particle size and morphology between the bulk materials and the RIVA-HESP cocrystal. The bulk RIVA appeared to consist of large, bladed slats, varying in size between 10-50µm. Meanwhile the HESP cofomer is made up of irregularly shaped, angular structures. A vast reduction in particle size is seen for the RIVA-HESP cocrystals, with the majority of particles being below 1.0µm in size. In addition, the cocrystal samples are mostly spherical and appear to have agglomerated into a more structured framework.



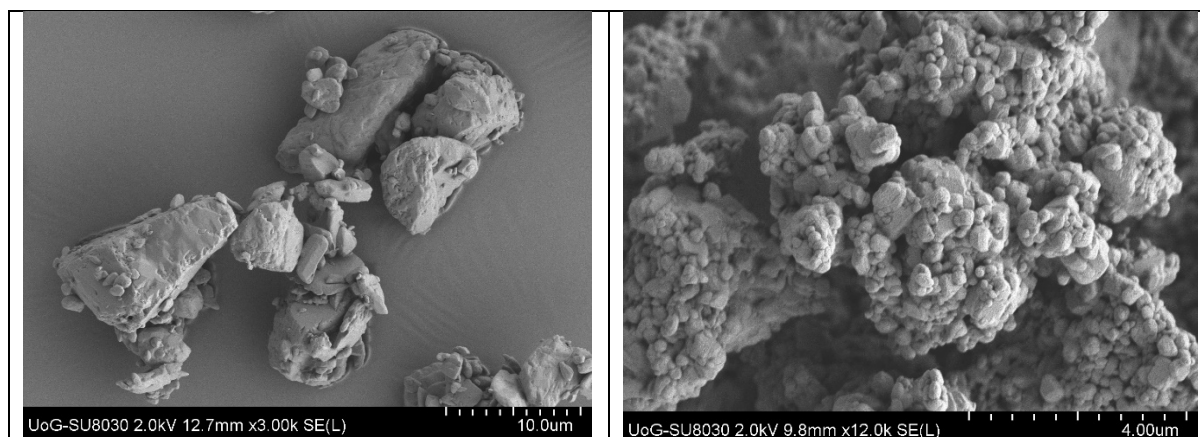


Figure 3: Images Bulk RIVA (top left), Bulk HESP (bottom left) and PER-SACC Cococrystal from two different magnifications (right).

4) Product #4: Carbamazepine–Naproxen Cococrystal

A new solid entity has been synthesized from carbamazepine (CBZ) and naproxen (NAP), two crystalline compounds, by Liquid Assisted Grinding (LAG). For this, a physical mixture of CBZ and NAP was prepared with a 1: 1 molar ratio. The mixture was ground at room temperature, after adding 20 μ L of methanol, at a frequency of 30 Hz for a total of 30 min (6 times 5 min of grinding with 5 min pause in between each to avoid any overheating of the mixture). The new solid entity obtained is a cococrystal, denoted CBZ: NAP , which has been characterized by PXRD, TGA and DSC.

Calorimetric analyses.

TGA analysis of the new entity CBZ:NAP, Figure 1, shows that there is no phenomenon occurring before 120 ° C. This confirms that there are no residues of the solvent used during the grinding of the physical mixture or that there has been no absorption of water made by the compound during its synthesis and/or storage time. The beginning of a mass loss due to the passage to the gas phase is perceptible around 120 ° C. This loss of mass happens in two stages,



between 120 °C and 250 °C, where 97% of weight is lost abruptly, then the remaining 3% is lost between 250 °C and 300 °C. It can be concluded that the new compound CBZ: NAP is thermally stable at least up to 120 °C.

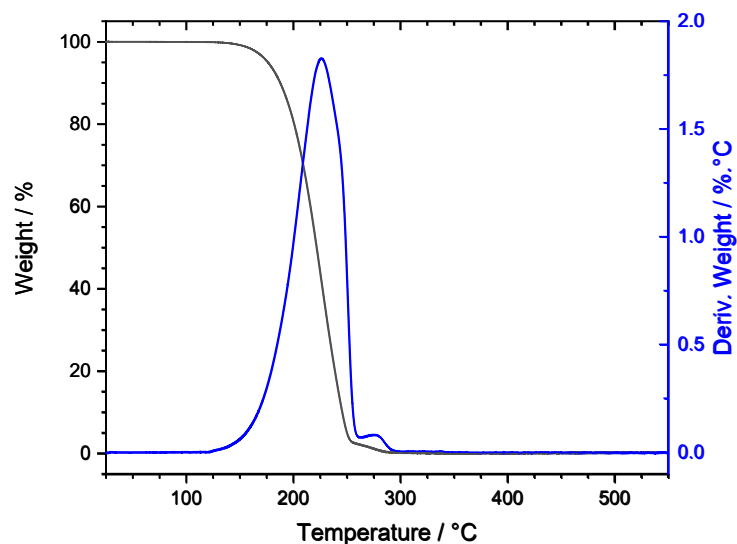


Figure 1 – TGA analysis (at 5 K.min⁻¹) of the new entity CBZ:NAP showing the thermal stability of the compound between room temperature and 120 °C.

First of all, a DSC analysis of the new compound CBZ:NAP was carried out at a heating rate of 20 K.min⁻¹ and compared to the pure compound DSC analysis performed under the same conditions. As it is shown in Figure 2, the cocystals thermogram shown only one endothermic peak (not traces of the pure compound are seen), which indicates that the new entity is in the crystalline state and it is chemically pure. The compound is characterized by a melting peak at $T_m^{CBZ:NAP}=125$ °C, which demonstrates a decrease of the melting temperature compared to both pure compounds ($T_m^{NAP}=155$ °C and $T_m^{CBZ(III)}=176$ °C / $T_m^{CBZ(I)}=191$ °C). Given these results, and considering that a lower melting point can mean a higher solubility of the compound, the solubility of the cocystal could show an improvement compared to the very low solubility in water of naproxen (15.9 mg.L⁻¹ at 25 °C²²) and carbamazepine (~17 to 150 mg.L⁻¹ at 25

°C²²), both of which are compounds considered to be slightly soluble in water. Table 1 summarizes the thermal characteristics of the cocrystal CBZ:NAP and the crystalline pure compounds (CBZ and NAP) used for the synthesis.

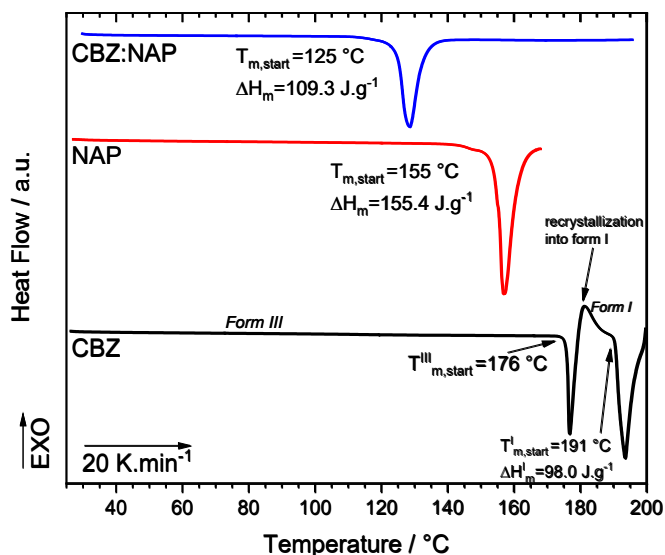


Figure 2 - DSC analyses of the new cocrystal CBZ:NAP and the pure crystalline compounds CBZ and NAP at a heating rate of 20 K.min⁻¹.

Table 1 – Thermal properties of the new cocrystal CBZ:NAP vs. the pure crystalline compounds. T_m=starting temperature of the melting peak.

	Melting temperature T _m / °C	Fusion Enthalpy ΔH _f / J.g ⁻¹	Fusion Entropy ΔS _f / J.mol ⁻¹ .K ⁻¹
Carbamazepine forme III	176 °C	N.A.	N.A.
Carbamazepine forme I	191 °C	109.2 +/- 1.5	55.5 +/- 0.8
Naproxen	155 °C	137.1 +/- 12.1	73.5 +/- 6.5
CBZ:NAP(1 :1)	125 °C	104.9 +/- 6.6	61.7 +/- 4.2

For a more complete calorimetric analysis of the new compound, a heating run (1) at 5 K.min⁻¹ was carried out from 20 °C to 140 °C (start of transition to vapor state or degradation, 0.4% loss of mass at this temperature from the TGA analysis), followed by cooling of the molten compound from 140 °C to -70 °C at 20 K.min⁻¹ then finally, a second heating (2) from -70 °C to 140 °C at 5 K.min⁻¹. It is interesting to note that during cooling, no sign of crystallization was observed, which shows the possibility for the liquid of CBZ: NAP to amorphize in opposite to the pure products. In the same cooling conditions it is impossible to obtain a glass of pure CBZ or of NAP. The result of this DSC analysis can be seen in Figure 3(only the thermograms obtained during heating are shown).

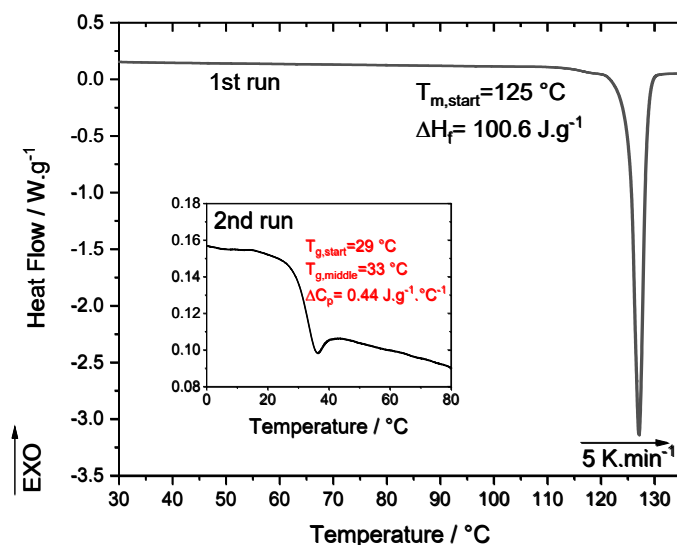


Figure 3 – DSC thermograms of the new entity CBZ: NAP recorded during two heating runs at 5 K.min⁻¹. Run 1 : melting of the cocrystal CBZ: NAP obtained by LAG. Run 2 (inset) : C_p jump characteristic of the glass transition of the new entity CBZ: NAP obtained in the amorphous state by cooling down to -70 °C (at 20 K.min⁻¹) of the molten compound (run 1) . (See details in the text)

In Figure 3, we can observe a melting peak (run 1) with a temperature and enthalpy of fusion in agreement with the values obtained at 20 K.min⁻¹. It should be noted that there is no clear evidence of degradation during heating to 140 °C, therefore, the loss of mass observed in ATG (0.4%) would most likely be due to the evaporation of the sample. The inset clearly shows that it was possible to obtain a glass by cooling the molten CBZ:NAP compound. This also constitutes another original result of this invention. With regard to the glass transition T_g of the compound CBZ:NAP, a glass transition temperature value T_g is obtained at the start of the jump of C_p of T_g = 29 °C, with a value of ΔC_p of 0.44 J.g⁻¹.°C⁻¹.

Figure 4 shows the corresponding X-ray diffractograms of the new system CBZ:NAP (blue) and of the pure compounds used for the synthesis, CBZ (black) and NAP (red). The diffractogram of the cocrystal CBZ:NAP shows new peaks distinguishing a new entity, the CBZ:NAP shows distinctive peaks not corresponding to those of the pure compounds and it does not show any peak corresponding to CBZ nor NAP. These results confirm that a new pure crystalline multicomponent system of CBZ: NAP was obtained by LAG.

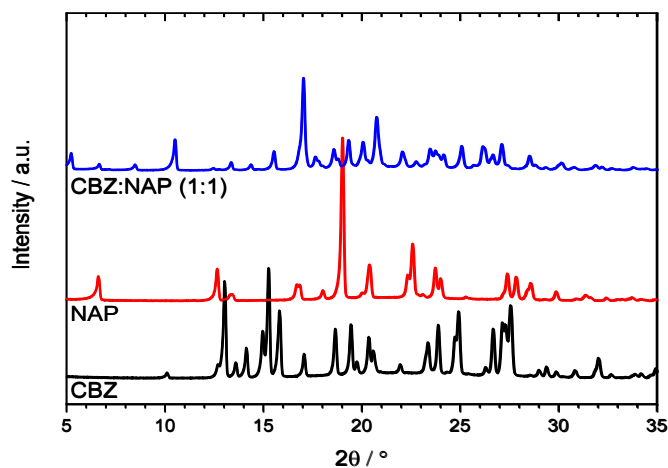


Figure 4 – XRD diffractograms of the new entity CBZ:NAP obtained by LAG vs. the pure compounds (CBZ and NAP).

REFERENCES

- 1 A. T. M. Serajuddin, *Adv. Drug Deliv. Rev.*, 2007, **59**, 603–616.
- 2 P. Cerreia Vioglio, M. R. Chierotti and R. Gobetto, *Adv. Drug Deliv. Rev.*, 2017, **117**, 86–110.
- 3 J. Wouters and L. Quéré, *Pharmaceutical Salts and Co-crystals*, The Royal Society of Chemistry, 2011.
- 4 C. B. Aakeröy, M. Fasulo, N. Schultheiss, J. Desper and C. Moore, *J. Am. Chem. Soc.*, 2007, **129**, 13772–13773.
- 5 D. Cinčić, T. Friščić and W. Jones, *Chem. - A Eur. J.*, 2008, **14**, 747–753.
- 6 B. K. Saha, A. Nangia and M. Jaskólski, *CrystEngComm*, 2005, **7**, 355–358.
- 7 N. Suzuki, M. Kawahata, K. Yamaguchi, T. Suzuki, K. Tomono and T. Fukami, *Drug Dev. Ind. Pharm.*, 2018, **44**, 582–589.
- 8 Y. Yuliandra, E. Zaini, S. Syofyan, W. Pratiwi, L. N. Putri, Y. S. Pratiwi and H. Arifin, *Sci. Pharm.*, 2018, **86**, 1–11.
- 9 E. Skorupska, S. Kaźmierski and M. J. Potrzebowski, *Mol. Pharm.*, 2017, **14**, 1800–1810.
- 10 S. Kudo and H. Takiyama, *J. Cryst. Growth*, 2014, **392**, 87–91.
- 11 I. C. Wang, M. J. Lee, S. J. Sim, W. S. Kim, N. H. Chun and G. J. Choi, *Int. J. Pharm.*, 2013, **450**, 311–322.
- 12 M. B. Hickey, M. L. Peterson, L. A. Scoppettuolo, S. L. Morrisette, A. Vetter, H. Guzmán, J. F. Remenar, Z. Zhang, M. D. Tawa, S. Haley, M. J. Zaworotko and Ö. Almarsson, *Eur. J. Pharm. Biopharm.*, 2007, **67**, 112–119.
- 13 D. Hasa and W. Jones, *Adv. Drug Deliv. Rev.*, 2017, **117**, 147–161.
- 14 W. W. . Porter III, S. C. Elie and A. J. Matzger, *Cryst. Growth Des.*, 2008, **8**, 14–16.
- 15 R. Thakuria, A. Delori, W. Jones, M. P. Lipert, L. Roy and N. Rodríguez-Hornedo, *Int. J. Pharm.*, 2013, **453**, 101–125.
- 16 D. D. Bavishi and C. H. Borkhataria, *Prog. Cryst. Growth Charact. Mater.*, 2016, **62**, 1–8.
- 17 N. J. Babu and A. Nangia, *Cryst. Growth Des.*, 2011, **11**, 2662–2679.
- 18 S. L. Childs, N. Rodríguez-Hornedo, L. S. Reddy, A. Jayasankar, C. Maheshwari, L. McCausland, R. Shipplett and B. C. Stahly, *CrystEngComm*, 2008, **10**, 856–864.
- 19 D. Hasa, E. Miniussi and W. Jones, *Cryst. Growth Des.*, 2016, **16**, 4582–4588.
- 20 C. Pando, A. Cabañas and I. A. Cuadra, *RSC Adv.*, 2016, **6**, 71134–71150.
- 21 S. Aher, R. Dhumal, K. Mahadik, A. Paradkar and P. York, *Eur. J. Pharm. Sci.*, 2010, **41**, 597–602.
- 22 S. H. Yalkowsky, Y. He and P. Jain, *Handbook of Aqueous Solubility Data*, 2nd edn.

C) Design of others cocrystal compounds using liquid assisted grinding and solution evaporation (Carbamazepine– DL-tartaric acid, Carbamazepine – L-tartaric acid)

Cocrystal of Carbamazepine– DL-tartaric acid and Carbamazepine – L-tartaric acid

EXPERIMENTAL SECTION

I. Materials:

Carbamazepine was obtained from Duchefa Farma BV. DL-tartaric acid and L-Tartaric acid were purchased from Sigma-Aldrich. All reagents were used as received.

II. Multicomponent systems:

The multicomponent systems (CBZ:DL-TA and CBZ:L-TA) were obtained using two different cocrystallization methods by solution evaporation (Sol) and by Liquid Assisted Grinding (LAG). Different molar ratios were tried out.

- i. **Solution evaporation:** A physical mixture of API and coformer was totally dissolved into methanol under continuous stirring. Then the solvent was left to evaporate at room temperature until the crystallized powder was dried.
- ii. **Liquid Assisted Grinding:** A Mixer Mill MM 400 from Retsch was used to grind the different physical mixtures adding a minimal volume of solvent (20 μ L of methanol for 200mg of mixture) into the mixture before grinding. The mixtures were ground for a total time of 30 min at room temperature by doing 6 cycles of 5 min milling with 5 min of interval between each cycle in order to avoid any possible overheating of the sample.

III. Characterization techniques

- i. **Differential Scanning Calorimetry (DSC).** Calorimetry characterization was done at the UMET at Université de Lille, France. A DSC from TA Instruments Inc, the Q1000 (from -90 to 230 °C) was used. Samples (2-3 mg of API) were placed in a hermetic aluminum sample cell (some of them with a pinhole) and the DSC measurements were carried out at 5K.min⁻¹ heating rates under a highly pure nitrogen atmosphere with a sample purge flow rate of 50 mL.min⁻¹. The temperature readings were calibrated using an indium standard.
- ii. **X-Ray Powder Diffraction (PXRD).** Powder X-Ray diffraction analysis was carried out with a PANalytical X'Pert pro MPD diffractometer equipped with a Cu X-ray tube (selected wavelength $\lambda_{\text{CuK}\alpha} = 1.54056 \text{ \AA}$) and the X'celerator detector. The samples were enclosed in a Lindemann glass capillary (diameter 0.7 mm) which was rotated during the experiments. The measurements were performed in transmission mode with incident beam parabolic mirror.
- iii. **Dielectric Relaxation Spectroscopy (DRS).** The complex dielectric function $\varepsilon^*(f) = \varepsilon'(f) - i\varepsilon''(f)$, where f is the frequency of the applied oscillating electrical field and ε' and ε'' are the real and imaginary parts, respectively. Measurements were carried out from 10⁻¹ to 10⁷ Hz using a high-resolution ALPHA analyzer. Samples were prepared in parallel plate geometry between two gold-plated electrodes with a diameter of 10 mm. The samples were previously cooled to -150 °C with a "Newtonian" cooling rate. Dielectric spectra were collected isothermally from -130 to 100 °C in increasing steps of 5 °C. A first heating

procedure is performed in order to dry the sample. Then the sample is cooled again to $-130\text{ }^{\circ}\text{C}$ for a second isothermal heating procedure until $100\text{ }^{\circ}\text{C}$. The temperature of sample was regulated using a Quatro cryo-system nitrogen flux device that keeps temperature fluctuations within $0.2\text{ }^{\circ}\text{C}$. Data analysis are done on the second run in order to probe the dynamics without the water influence.

RESULTS AND DISCUSSIONS

Cocrystallization trials between CBZ and DL-TA were performed using two synthesis methods: solution evaporation (Sol) and liquid assisted grinding (LAG). Firstly, a molar ratio of 1 to 1 was used. The obtained results are shown in Figure 1.

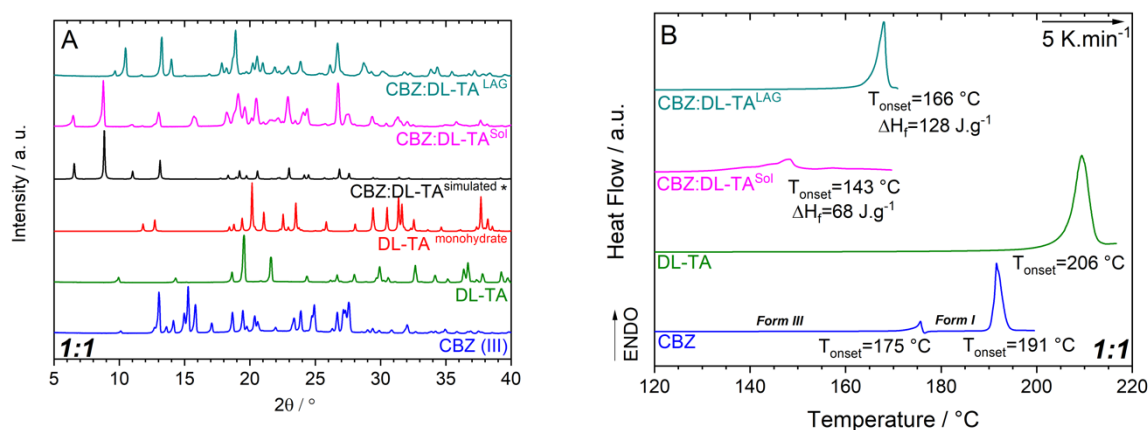


Figure 5 - Cocrystallization trials at (1:1) ratio between CBZ and DL-TA. (A) PXRD patterns of the pure compounds and the obtained results from LAG and solution evaporation, (B) DSC results of the pure compounds and the obtained results.

The DSC and XRD analyses of the obtained compounds (Figure 1) showed that two different cocrystals were obtained, one by LAG ratio 1:1 (teal curve) and one that has already been published in the Cambridge Data base (CSD) with an unknown ratio (pink curve). This compounds will be named CC1 and CC2 respectively in the following report.

I. CC1

The cocrystallization of carbamazepine with DL-TA using liquid assisting grinding showed by XRD and DSC analyses no sign of the pure compounds, therefore, a pure cocrystal that has not been yet published in the CSD was obtained. For this reason, the resolution of the structure was performed using powder X-ray diffraction thanks to the help of Dr. Mathieu GUERAIN and Dr. Patrick DEROLLEZ. The structural resolution details are shown below.

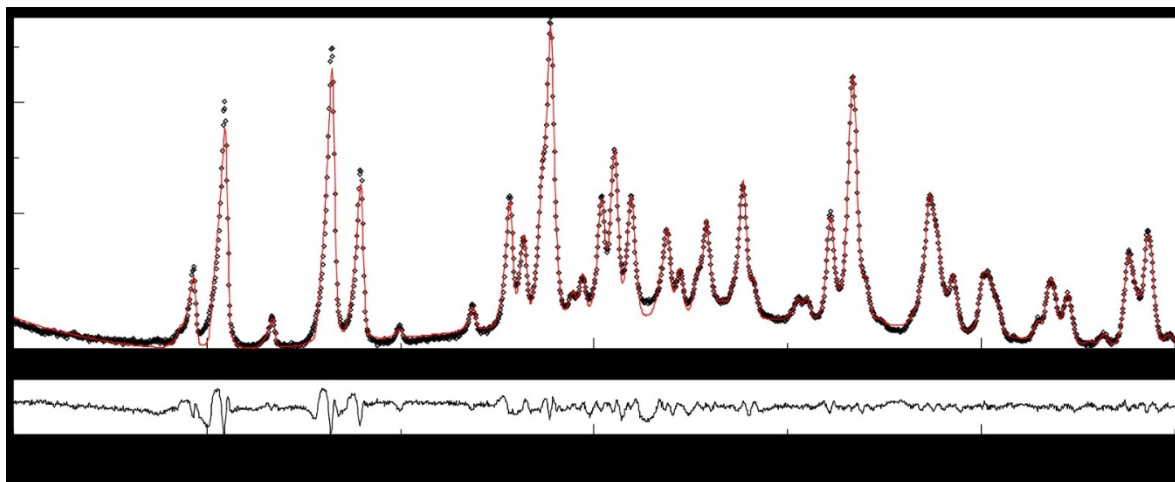


Figure 6 – Rietveld refinement of the CBZ+DL-TA cocrystal ratio 1:1 obtained by LAG. (black line is the real diagram and in red is the refined one).

Table 2 – Crystallographic data, profile and structural parameters for CBZ/DL-TA cocrystal obtained after Rietveld refinements.

Crystal data	
Chemical formula	C ₁₅ H ₁₂ N ₂ O, C ₄ H ₆ O ₆
M _x	386.4
Cell setting, space group	Monoclinic, P 2 ₁ /c
Temperature (K)	293
a,b,c (Å)	4.96281 (9), 9.3761 (3), 37.8966 (9)
β(°)	92.9617(17)
V (Å ³)	1761.05 (7)
Z	4
F (000)	808
μ (mm ⁻¹)	0.043
Specimen shape, size (mm)	Cylinder, 0.5
2θ range (°)	0.5 – 27.9°
Data collection	
Beamline	ID22 (ESRF)
Specimen mounting	0.5 mm diameter Lindemann capillary
Data collection mode	Transmission (Debye-Scherrer geometry)
Scan method	Continuous scan
Radiation type	Synchrotron 31 KeV, λ= 0.39997 Å
Binning size (° 2θ)	0.0015
Refinement	
R factors and goodness of fit	R =0.0980, R _{wp} _{nb} =0.1302, R _{exp} = 0.0732
No. of refined parameters	108

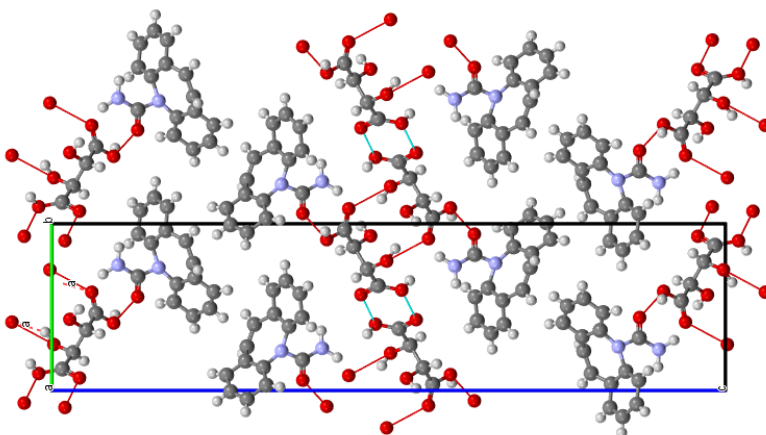


Figure 7 - Projection of the unit cell along the [001] direction for CCG cocrystal

II. CC2

i. Ratio trials

The CBZ:DL-TA^{Sol} (pink curve in Figure 1) system at a 1:1 molar ratio cocrystallization trial showed that the obtained compound is a mixture of a published cocrystal and DL-TA monohydrate. As no rest of carbamazepine form III or any other polymorph (or hydrate) was found in the substance, it means that all the carbamazepine was used for the cocrystallization with DL-TA. Therefore, the 1:1 ratio used for this cocrystallization does not correspond to a pure cocrystal.

In parallel to the cocrystallization trials of CBZ with DL-TA, cocrystallization trials using L-TA as a coformer were performed as well. The exact same conditions as the DL-TA cocrystallization were used for both methods, Sol and LAG.

The main result concerning the cocrystallization trials of the system CBZ:L-TA is that both methods used for the synthesis converge into the same cocrystal, CC2. Indeed, the cocrystallization trials with this coformer did not show any sign of the second cocrystal, CC1, obtained with DL-TA by LAG at a molar ratio of 1:1. Only the results for CBZ:L-TA system cocrystallized by LAG will be shown in this report.

The powder diffraction diagrams obtained for the different systems were treated using the Rietveld method thanks to the MAUD (Materials Analysis Using Diffraction) software. For this quantitative analysis of the cocrystal, cocrystallization trials of CBZ with L-TA were prepared from LAG and solution evaporation in different ratios: (1:1), (2:1), (3,1), (4,1) and (5:1).

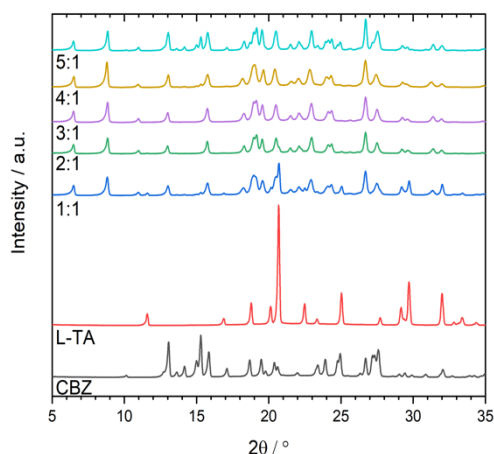


Figure 8 – PXRD patterns of the different molar ratio trials for the CBZ:L-TA cocrystallized by LAG compared to the pure compounds.

All of the data obtained was analyzed using the Rietveld method and the results of these analyses are shown in Table 2. It should be noted that the CIF documents used for the fitting of the curves were taken from the CSD including the one for CC2, as it is the only existing CIF file for CC2.

Table 2 corresponds to the quantification of the diagram shown in Figure 4. the results obtained with the CBZ:L-TA system cocrystallized by LAG,, carbamazepine varies between 0.02 and 3.8 %, the first 3 ratios are lower than 1.5 %, then this percentage increases to 3.8 and for the 5:1, the carbamazepine percentage value explodes to 47 % of pure CBZ. In the meantime, the percentage of L-TA decreases from 35 to 0% in the first 4 ratios (therefore the percentage of cocrystal might not increase anymore), the CC2 % goes from 63.9 % to 98.4 % at its maximum (for the 3 to 1 ratio). Then, it decreases to 96.2 % for the 4 to 1 ratio (the same ratio as when the percentage of carbamazepine increases) and then it decreases to 52 % for the 5 to 1 ratio. From these results, the conclusion would be that the pure cocrystal is more a 3 to 1 ratio than a 4 to 1.

Table 3 - Quantification of CBZ:L-TA cocrystallization system at different molar ratios using the Rietveld Method.

CBZ+L-TA (LAG)			
Ratio	% CBZ	%L-TA	%CC2
1:1	1.1	35	63.9
2:1	0.02	16.5	83.4
3:1	1.3	0.3	98.4
4:1	3.8	0	96.2
5:1	47	0	52

Although the results have not been shown in this work, a final conclusion over the real molar ratio of CC2 has not been possible to reach, whether from solution or LAG cocrystallizations analyzed by PXRD. Indeed, the other cocrystallization results show different quantification percentages and there is a possibility that the real ratio is a 3:1 and not a 4:1 ratio.

As it was not possible to determine the exact ratio of this cocrystal by PXRD data and the DSC data is not any help in this matter, NMR spectroscopy was performed in two of the ratios 3:1 and 4:1 using the CC2 obtained from CBZ:L-TA using liquid assisted grinding. These analyses were performed in collaboration with Prof. Khimyak, University of East Anglia. The conclusions obtained from the NMR analyses were in agreement with the ones from PXRD data.

ii. NMR Analyses

Figure 6 shows the solid NMR analyses of the two cocrystallization trials. The pure compound L-TA shows a doublet at 72.7 ppm and 74.7 ppm. When compared to the cocrystallization results, it is possible to see that one of these peaks disappears when cocrystallization is done, confirming that a new entity is obtained from CBZ and L-TA. Furthermore, there is another doublet at 176.7 ppm and 172 ppm. This doublet also decreases, both of the peaks at the same time, with cocrystallization finishing in a single broad peak. Although it is not very precise as a result, it is possible to see that in this case, the doublet of the 4:1 ratio disappears more than the one from the 3:1 ratio as the one in the 4:1 sample has still a recognizable doublet and the one of the 3:1 could be taken as just one peak. This fact could mean that the pure CC2 is obtained from a 4:1 ratio and not a 3:1 ratio. Nonetheless, as it was made from PXRD analyses, it would be useful to compare also these results to the ones of pure CBZ and see if any rests of the pure compound are found in the 4:1 ratio. The problem with this is that carbamazepine is a compound that does not show a good response to the technique. Indeed, in order to obtain a good spectrum it would be necessary to do the analysis over a long period of time (at least a week), therefore it is very time consuming. A spectra acquisition was done for some hours but the resolution of the peaks was not good enough in order to compare to the spectra obtained from the cocrystals and see any differences that could help us to reach a conclusion.

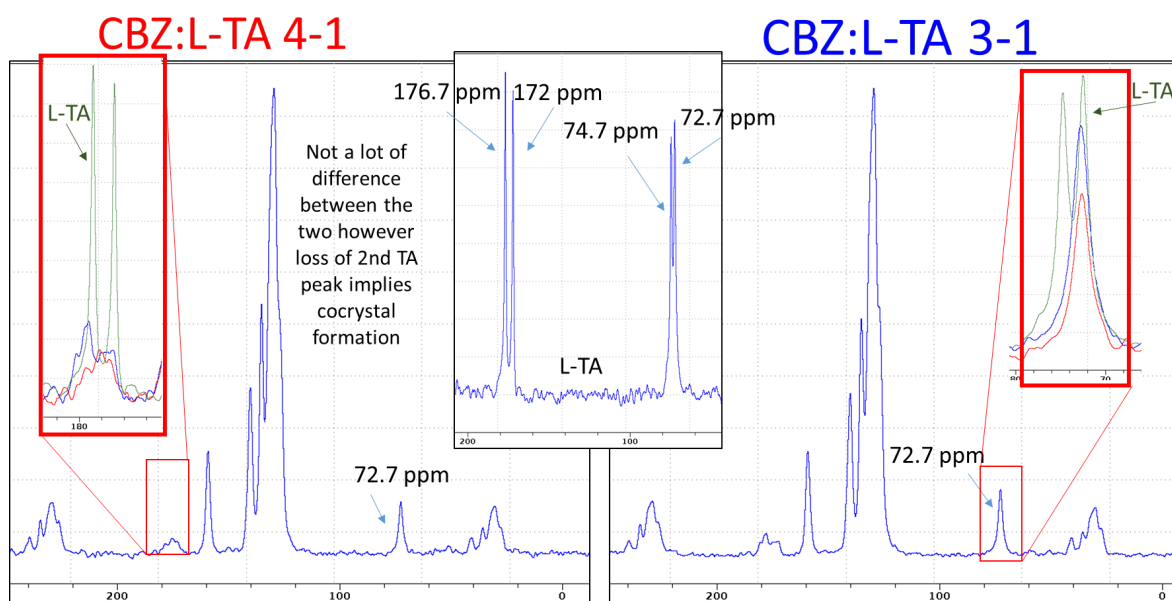


Figure 9 – NMR analysis of CC2 obtained from CBZ:L-TA (4:1) in the left and CBZ:L-TA (3:1) in the right. The results of the pure L-TA are shown in the middle, where characteristic peaks of this compound are highlighted. The inserts show the stacking of both cocrystallization trials CBZ:L-TA (4:1) in red and CBZ:L-TA (3:1) in blue along with the pure L-TA in green.

iii. DRS Results

Although Dielectric Resonance Spectroscopy is not a common technique used to characterize the crystalline state as this state normally does not show any response (amorphous disordered compounds are the usual samples used for this technique), there are some cases in which it can be interesting to see if a crystal compound shows any response by studying its response to the electric field applied by this technique, as for example caffeine¹. As it has been said before, the structural resolution made by Childs² was difficult as the position of the coformer in the crystalline structure could be statically disordered. Therefore, the cocrystal CC2 and the pure compounds were tested by DRS, the results are shown in Figure 8.

It is possible to see that the cocrystal (red) is showing a response as a relaxation peak appears. On the contrary, none of the pure compounds CBZ (blue) and L-TA (black) show a relaxation peak, which is the common response of a crystal in DRS. This allows us to conclude that the relaxation peak showed by CC2 does not correspond to a specific disorder coming from one of the pure compounds. The relaxation peak is a proof of the presence of a dynamical disorder of the cocrystal.

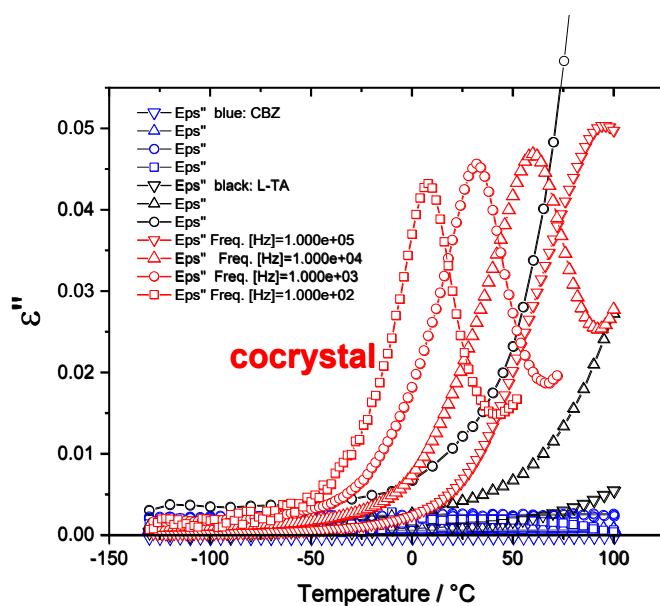


Figure 10 – DRS analysis of aged CC2 obtained from CBZ-L:TA (3:1) using the LAG method with anhydrous acetonitrile added. Comparison to the pure compounds CBZ and L-TA.

This result is very interesting as this cocrystal has not only a static disorder but also a dynamical disorder.

CONCLUSION

Two different cocrystals out of the CBZ:DL-TA system were obtained using two different synthesis techniques. The thermal and structural behavior of the obtained polymorphs were compared. One of them, CC1, obtained by LAG with a 1:1 molar ratio, corresponds to a cocrystal that has never been published in the CSD, having new physical and structural properties. The resolution of the structure was done.

The second one, CC2, was found to correspond to an already known polymorph from the literature and it is possible to obtain it using the isomer L-TA. This later, shows that it is not pure at a molar ratio of 1:1. Therefore, a

comparative study of the cocrystallization of CBZ:L-TA and CBZ:DL-TA systems were also performed for different ratios and no final conclusion was possible to make between the 3:1 and the 4:1 ratio neither from PXRD data nor from NMR studies.

The 3:1 compound was analyzed by DRS showing a relaxation peak. Therefore, the CC2 cocrystal shows a dynamical disorder.

REFERENCES

- 1 M. Descamps, N. T. Correia, P. Derollez, F. Danede and F. Capet, *J. Phys. Chem. B*, 2005, **109**, 16092–16098.
- 2 S. L. Childs, N. Rodríguez-Hornedo, L. S. Reddy, A. Jayasankar, C. Maheshwari, L. McCausland, R. Shipplett and B. C. Stahly, *CrystEngComm*, 2008, **10**, 856–864.

D) Development of new computational approaches for the screening of coformers for cocrystals screening

Affinity prediction computations based on the COSMO-RS approach of the Active Pharmaceutical Ingredient (API) carbamazepine have been performed with 75 coformers. A selection of coformers and cocrystallization trials by means of mechanosynthesis using liquid assisted grinding has been investigated. Two new cocrystals of carbamazepine with DL-mandelic acid and DL-tartaric acid and one new polymorph with indomethacin have been designed. The affinity predictions computations enabled to calculate the excess enthalpy ΔH_{ex} of the API-coformer mixture relative to the pure components. The ability of ΔH_{ex} to predict cocrystallization was assessed based on the new experimental results obtained in this study and data available in the literature. It is shown that affinity predictions computation might not be totally sufficient when it comes to the selection of all of the coformers that could cocrystallize with carbamazepine. A combination of the excess enthalpy ΔH_{ex} with the fusion entropy of the pure coformer is suggested to be of interest for coformers screening in order to form a multicomponent system with a given API (co-crystal/co-amorphous).

The full description of the computational approaches is described has been published in [Affinity prediction computations and mechanosynthesis of carbamazepine based cocrystals. L. Roca Paixao, N. T. Correia, F. Affouard, Crystengcomm (2019)] and it is provided in the annexes.

II) Description of the results obtained for the output in term of specific results category and specific result type

Specific results category And Specific result type	Description of the specific results
<p>Knowledge - Created/Increased skill and capacities</p>	<p>Based on the work performed in Output 2, we have published the following 4 articles while another 3 are under preparation (submissions on May 2020):</p> <ul style="list-style-type: none"> - 3D printed "Starmix" drug loaded dosage forms for paediatric applications. N. Scoutaris, S.A. Ross, M.J. Snowden, D. Douroumis. Pharm. Res. (2018) - Solid State Thermomechanical Engineering of High-Quality Pharmaceutical Salts via Solvent Free Continuous Processing. Md Mithu, S.A. Ross, B.D. Alexander, D. Douroumis. Green. Chem (2020) - Structure determination of Carbamazepine/DL-TA co-crystal by synchrotron powder X-ray diffraction. M. Guerain, P. Derollez, L. Roca Paixao, C. Dejoie, N. T. Correia, F. Affouard, , Acta Crystallographica Section C Structural Chemistry (2020) - Affinity prediction computations and mechanosynthesis of carbamazepine based cocrystals. L. Roca Paixao, N. T. Correia, F. Affouard, Crystengcomm (2019) <p>The work has been presented in several conferences (podium and poster presentations): Oxford Global (2019, UK), PharmSci (2019, UK), Symposium – QbD (2018, UK), Symposium – QbD (2019, UK), Formulation & Delivery (Oxford Global, 2019, UK), JPAG (2019, UK), CGOM13 (2018, South Korea)</p> <p>We have also delivered three webinars for Oxford Global and BioPharma Asia which attracted international audience from pharmaceutical industry</p>
<p>Socio-Economic -Increased business activities/capacities (new products, processes, services, techniques)</p>	<p>The developed technologies and novel drug cocrystals have been incorporated to Cubic Pharmaceuticals (PP10) portfolio and expected to enhance the company's competitiveness. Cubic has attracted strong interest for licencing the proprietary technologies and initiated discussions for future marketed products. The UoG (PP7) has contributed significantly to the development of those technology and continues to further collaborate with Cubic (PP10) for the development of new technologies or marketed pharmaceutical products.</p> <p>PP7, PP10 and LP12 have also contacted the following companies and communicated our research with them:</p> <ol style="list-style-type: none"> 1. SCI PHARMA, ALGERIA

	<ol style="list-style-type: none"> 2. SIMSON PHARMA LIMITED, INDIA 3. CHINA PHARMA SOLUTIONS, China 4. GATTEFOSSE, France 5. DURBIN PLC, UK 6. OMNICAL INDIA LIMITED 7. FARMALIDER 8. QUAY PHARMA, UK 9. LYRUS INDIA LTD 10. AMPLE LOGIC LTD 11. MEDREICH PHARMA, UK 12. ECZANE PHARMA, ARGENTINA 13. INSCG PHARMA 14. ALFA SIGMA PHARMA 15. UNITHER, France 16. CATALENT PHARMA SOLUTIONS, USA 17. ALFA SIGMA PHAMA 18. SPINOFRIN LIMITED 19. EMCURE PHARMACEUTICALS LTD, INDIA 20. JUBILANT PHARMACEUTICALS, INDIA 21. CHEMIFARM LTD, EGYPT 22. AINIA LIMITED 23. PROFILE HIT 24. BIOMATHEMATICA LTD 25. UNITHER PHARMA 26. CIL CARE 27. LAXAI PHARMA 28. SERVIER, France
<p>Socio-Economic -Patent applications</p>	<ul style="list-style-type: none"> - 2 patent have been filed through the collaboration of PP7 and PP10 by using patent solicitors (Venner Shipley, London, UK) - 1 Invention disclosure has been submitted by LP12 to the Tech Transfert Accelerator Network SATT-NORD (French side).

List of documents enclosed as annex
--

Images	None
Reports and high impact publications	4 high impact publications.
Communications in European and/ or international events	Oxford Global (2019), PharmSci 2019, Intrerpharm 2018, Cellink 2018, JPAG 2019
Patent prior art search & patent preparation	3 patents filed. 1 Invention disclosure.
Patent	None
Official letters from company(ies)	None